The Value of Time: Evidence from Auctioned Cab Rides*

Nicholas Buchholz† Laura Doval‡ Jakub Kastl§ Filip Matejka¶
Tobias Salz‖

June 10, 2022

Abstract

We recover valuations of time using detailed data from a large ride-hail platform, where drivers bid on trips and consumers choose between a set of rides with different prices and waiting times. Leveraging a consumer panel, we estimate demand as a function of both prices and waiting times and use the resulting estimates to recover heterogeneity in the value of time at the individual level. We study the welfare implications of platform pricing policies that take advantage of this heterogeneity. In particular, we compare the consumers', drivers', and platform's welfare under different forms of price discrimination. Taking into account drivers' optimal reaction to the platform's pricing policy, total surplus falls by 6% under personalized pricing relative to the current mechanism. However, total surplus grows by 33% compared to the case in which the platform does not incorporate consumer information into its pricing.

Keywords: Value of time, demand in transportation markets, ride hail, price discrimination.
JEL classification: C73; D83; L90; R12

*We thank the Editor, Aviv Nevo, and four anonymous referees for feedback that has greatly improved this paper. We thank Juan Camilo Castillo, Gabriel Kreindler, Rob Porter, Stephen Redding, and seminar participants at FTC, Maryland, MIT, Ohio State, Penn, Princeton, Stanford, UCL, WashU and IO^2 for useful comments. We thank Stefano Baratuche, Jacob Dorn, Thi Mai Anh Nguyen, Roi Orzach, and Yining Zhu for exceptional research assistance. We are grateful for the financial support from the Transportation Economics in the 21st Century Initiative of the NBER and U.S. Department of Transportation. Kastl is grateful for the financial support of the NSF (SES-1352305). All remaining errors are ours.

†Princeton University, 20 Washington Rd, Princeton, NJ 08540

‡Columbia University, 665 West 130th Street, New York, NY 10027

§Princeton University, 20 Washington Rd, Princeton, NJ 08540

¶CERGE-EI, Politickỳch vìzòù 7, 111 21 Prague 1

‖Massachusetts Institute of Technology, 50 Memorial Dr, Cambridge, MA 02142

1 Introduction

Credible measures of the value of time provide a key input to many economic analyses, particularly those surrounding the regulation and design of public and private transportation markets.[1] A unique empirical challenge to measuring the value of time is that time is not directly priced in many economic settings (Becker, 1965). In this paper, we use detailed consumer choice data from a large European ride-hailing platform, Liftago, to measure consumers' value of time and quantify the welfare effects of platform pricing policies that exploit the underlying heterogeneity in consumers' value of time.

To credibly measure the value of time, we exploit the unique features of Liftago's ride allocation mechanism, which allows consumers to directly express preferences over prices and waiting time – the time it would take a taxi to pick up the consumer.[2] Liftago allocates rides through a rapid auction process in which nearby drivers bid on ride requests. Requesting consumers then choose between bids based on various characteristics. Most importantly, bids often involve a trade-off between price and waiting time, allowing us to observe how consumers resolve this trade-off.

We make two primary contributions. First, relying on the unique features of our setting, we obtain estimates of the heterogeneity in the value of time across people on the platform by estimating a demand system that depends on both prices *and* waiting times. We observe consumers' individual choice sets as well as their ultimate selection for 1.9 million ride requests and 5.2 million bids. We also observe a consumer panel identifier that allows us to recover persistent differences in the value of time across consumers. Second, we use these estimates to quantify the welfare effects of platform pricing policies that exploit the heterogeneity in consumers' value of time to price discriminate. As we explain below, an important piece of this exercise is a model of driver behavior, which allows us to infer drivers' opportunity cost of serving a ride from their bidding behavior.

Our demand results quantify how much consumers respond to changes in both price and waiting time. Price elasticities are four to ten times as large as waiting-time elasticities. We find that on average consumers' willingness to pay for waiting time savings, expressed as an hourly quantity, is \$13.47. We refer to this quantity as the *value of time* (henceforth VOT). Furthermore, although these measures vary widely within the day and across space, most of the variation is driven by latent differences across riders independent of observable sources of variation. Ranking individuals by their relative sensitivity to prices and wait times, we find that the top quartile have VOT measures about 3.5 times higher than the bottom quartile.

[1] See, for instance, Belenky (2011) for the regulation and design of transportation markets, Arnott et al. (1993) for congestion pricing, and Freund and van Ryzin (2021) for surge-pricing in ride-hailing platforms.

[2] As we later show, Liftago's mechanism stands in contrast to that of platforms like Uber and Lyft, which employ "surge" pricing to equilibrate demand and supply.

The large heterogeneity we document in consumers' value of time raises the question of whether ride-hailing platforms can benefit from price discriminating on this basis. Section 6 studies the welfare effects of platform pricing strategies that exploit the heterogeneity in consumers' preferences over time and money. While individual values of time are not *directly* observed, platforms can take advantage of repeated interaction with consumers to learn their individual preferences. We explore the platform's benefit of using consumers' historical data as an input to pricing by analyzing the impact of different forms of price discrimination on consumer welfare and platform profits. Because the welfare effects of such pricing strategies is ambiguous, they are the subject of recent policy debates as firms gain access to more abundant consumer data.[3] We model the platform as procuring drivers through driver selection rules that resemble the baseline auction format. In contrast to the current platform policy, where the platform collects a percentage fee and directly implements drivers' bids as prices, we allow the platform to directly choose the price the rider faces.

An important piece of our counterfactual exercise is the estimation of a model of driver bidding. A unique aspect of platform price discrimination is that whenever the platform sets prices, drivers have the opportunity to react through their own prices, thereby endogenizing the platform's procurement costs. Thus, drivers' pricing behavior acts as a constraint on the ability of the platform to benefit from price discrimination. As a result, how additional surplus will be split between the platform and the drivers is not immediately clear. To the best of our knowledge, we are the first to highlight this supply-side friction on platform price discrimination and quantify its effects on a platform's profits.

To evaluate drivers' reactions and the resulting welfare consequences, we pose and estimate a model of drivers' bidding behavior on the platform to infer drivers' opportunity cost of serving a ride. In choosing their bids, drivers weigh the revenues from a trip against the value of their outside option, while also taking into account the dynamic implications of a trip, which might bring them to a more or less desired destination. Bids in the market thus reflect both drivers' heterogeneous outside options and the differences in the continuation values of winning an auction or not. To recover these opportunity costs, we adopt methods from the empirical auction literature (Guerre et al., 2000; Jofre-Bonet and Pesendorfer, 2003) that allow us to link the observed bids to the dynamic problem that drivers solve.

Having estimated the platform's demand and supply of rides, we quantify the welfare effects and the platform's profits of four different pricing policies: (i) uniform pricing, where the platform's pricing is common to all consumers; (ii) third-degree price discrimination, where the platform may choose different prices as a function of time of day or location; (iii) menu pricing, where the platform offers the consumer a menu containing the ride closest to the consumer; and (iv) personalized pricing, where the platform tailors consumer prices to all the data the platform

[3] See, for example, 2015 White House Brief, 2016 OECD Roundtable on Price Discrimination — Note by the United States, and 2018 OECD Brief on Personalised Pricing in the Digital Era.

has about that consumer. In order to measure the *shadow* cost imposed by drivers' endogenous behavior on the platform, we conduct our counterfactual exercise under two scenarios. In the first (*no driver adjustment*), the platform faces the same bid distribution as in the baseline. In the second (*driver adjustment*), we allow the drivers to optimally react to the platform's pricing policy. The comparison of the platform's profits across these two scenarios represents the limits that the drivers' endogenous behavior imposes on the ability of the platform to profit from more sophisticated pricing policies.

We show that the value to the platform of leveraging consumer information is substantial: under no driver adjustment, personalized pricing leads the platform to collect over 3.4 times the profits of the current mechanism, or about 2.7 times the profits from uniform pricing. When drivers optimally react to the platform's pricing policy, the platform still benefits from incorporating consumer information into its pricing, but platform profits decrease by 15%-25% relative to the case with no driver adjustment. Under the different pricing policies, the platform's profit increase follows from an increase in average prices per order and hence a decrease in the number of rides served by the platform.

Conditional on the platform using its pricing power, we show that both consumers and drivers fare better when the platform leverages its consumer information. Under no driver adjustment, consumer and driver surplus decrease by 37% and 57% under uniform pricing, respectively, relative to the current mechanism. However, relative to uniform pricing, personalized pricing increases driver and consumer surplus: trip volume nearly doubles relative to uniform pricing as price discrimination allows the platform to serve marginal consumers at lower prices, without sacrificing revenues on other trips. Once we incorporate drivers' reactions to the platform's pricing rule, welfare conclusions are more nuanced: the drivers and not the consumers are the ones who capture the gains from the platform incorporating more consumer information into its pricing mechanism. Both drivers and consumers are worse off under personalized pricing than under the baseline competitive auction mechanism, but the drivers benefit from the platform's increased use of information relative to uniform pricing.

Our results highlight the nuanced welfare effects of incorporating detailed consumer information into pricing, especially in two-sided markets. Relative to the competitive baseline mechanism where prices are set via auctions, our uniform pricing counterfactual shows there is unexercised pricing power by the platform, which comes at a considerable welfare cost for consumers and drivers. However, conditional on the platform exercising this pricing power, the more information the platform incorporates into its pricing mechanism, the more driver and consumer surplus is enhanced. Furthermore, our results highlight that our welfare conclusions depend on what side of the market we look at: once we account for drivers' optimal reactions, drivers command a substantial share of the surplus created by using more consumer information.

Related literature The paper contributes to four strands of literature, which we describe below.

The first strand is the literature on the opportunity cost of time starting with the work of Becker (1965). Recent papers in this literature use a variety of widely available micro-data to study the trade-off between market goods and time (see, for instance, Aguiar and Hurst, 2007; Aguiar et al., 2012; Nevo and Wong, 2019).[4] Our work contributes to this literature in a number of ways. We extend the analysis of the opportunity cost of time outside of the workplace and study how this value varies across individuals, locations, and time.

The second strand is the empirical literature on price discrimination that measures the benefits of second degree (Miravete, 1996; Hendel and Nevo, 2013; Luo et al., 2018) and third degree (e.g., Hendel and Nevo, 2013; List, 2004; Bauner, 2015; Levitt et al., 2016) price discrimination, as well as different forms of nonlinear and personalized pricing (e.g., Rossi et al., 1996; Shiller, 2013; Nevo et al., 2016; Dubé and Misra, 2019). Personalized pricing has gained additional importance in this era of large-scale data collection by platforms, particularly since the theory is ambiguous about its welfare and distributional effects.[5] Like Dubé and Misra (2019), we find evidence that the platform is not pricing optimally. In contrast to most of these papers, we study the question about the benefits of price discrimination in the context of a two-sided platform, exploiting that the platform's auction mechanism allows us to infer how consumers trade off waiting time and money when deciding amongst different trips.

The third strand is the literature in transportation economics and industrial organization, dating to the pioneering work of Daniel McFadden (McFadden, 1974; Domencich and McFadden, 1975), on the value of travel-time savings. These studies measure the benefits of travel-time savings through surveys or revealed preference analysis based on mode choice. Our data allow us to directly measure consumers' willingness to pay for reductions in waiting time based on choices on the platform. Although our willingness-to-pay measure is distinct from the value of travel-time savings, the two quantities are related. Small (2012) reviews the travel-time literature and presents stylized facts suggesting that the value of personal travel time is about 50% of the gross wage rate, and that the value of travel time increases less than proportionally with income/hourly wage — with elasticity estimates ranging from 0.5 to 0.9. Using an experimental approach, Goldszmidt et al. (2020) provide recent evidence on the value of time based on Lyft orders in the US. Aside from differences in the setting and methodology, a key distinction is our focus on platform pricing strategies.

[4] A related question is how much workers value flexible work schedules. Mas and Pallais (2017) investigate preferences for flexibility in an experiment with call-center workers, Bloom et al. (2015) study work-from-home preferences and performance differences among workers in a large travel agency. The taxi and ride-share industry has long provided a laboratory for empirical work on flexible work hours. See, e.g., Camerer et al. (1997), Farber (2005), Farber (2008), Crawford and Meng (2011),Thakral and Tô (2017), and Chen et al. (2017).

[5] The literature on the welfare effects of price discrimination goes all the way back to the seminar work of Pigou (1920); see Aguirre et al. (2010) and Bergemann et al. (2015) for recent studies. Some recent papers study this issue in the context of big data; see, for instance, Ali et al. (2020) for the benefits of voluntary disclosure of data, Kehoe et al. (2018) for personalized pricing in the market of experience goods, Aridor et al. (2021) for the effects of privacy protecting policies, and Doval and Skreta (2021) for how consumers' forward looking behavior affects the incentives of firms to collect data in the first place.

Recent studies of commuter behavior have also evaluated the value of time in various contexts. Couture et al. (2018) study the determinants of driving speed and the deadweight loss of travel, where hours in traffic are valued at half the average wage. Bento et al. (2020) use commuter tollway choices to infer consumers' urgency from their willingness to pay for travel time savings. Hall (2018) analyzes the benefits of choice over toll and non-toll lanes. Kreindler (2018) experimentally measures the value of peak-congestion pricing in Bangalore.[6]

The fourth strand is the literature that studies taxi and ride-hail markets. Buchholz (2018) quantifies the impact of uniform pricing regulation and search frictions on the spatial allocation of drivers and consumers in the NYC taxi market; Frechette et al. (2018) assess the effect of entry restrictions and market thickness on efficiency in the NYC taxi market.[7] In these papers, the demand for taxis is estimated either as a function of prices (Buchholz, 2018) or waiting times (Frechette et al., 2018), but not both.[8] Cohen et al. (2016), Castillo (2019), Rosaia (2020), and Gaineddenova (2021) estimate demand for rides on ride-hail platforms. In particular, Castillo (2019) and Rosaia (2020) also estimate demand for rides as a function of both waiting time and price. Castillo (2019) focuses on quantifying the benefit of surge pricing, and Rosaia (2020) studies economies of density. In our demand-side analysis, we observe direct choices over prices and waiting times and focus specifically on measuring these two elasticities. We also observe a panel of riders, which provides a convincing way to estimate population heterogeneity. Gaineddenova (2021) shows that a ride-hailing platform may obtain higher profits if instead of centralizing pricing decisions, it would allow consumers to bid on rides.

Organization The rest of this paper proceeds as follows. Section 2 describes the institutional setting and our data. Section 3 describes the conceptual framework and the model of consumer choice that we estimate. Section 4 describes the model of driver bidding, its identification, and estimation. Section 5 presents our estimation results. Section 6 analyzes different forms of price discrimination on the platform. Section 7 concludes.

2 Setting and Data

2.1 A Unique Approach to Matching and Price Discovery

Liftago is a ride-hail platform that was founded in 2015 and services rides through licensed taxi drivers. In Prague, all taxis need to be operated by licensed drivers. Licensing requires

[6] There are a host of other studies. See, e.g., Belenky (2011), Miller (1989), Abrantes and Wardman (2011), Cirillo and Axhausen (2006), Jara-Diaz et al. (2008). Borjesson et al. (2012) and Fosgerau et al. (2007).

[7] In a similar vein, Liu et al. (2019) and Hall et al. (2019) study various aspects of the design of DiDi and Uber, respectively. These papers, however, do not estimate demand.

[8] Brancaccio et al. (2017) and Brancaccio et al. (2020) study closely related models in the context of the oceanic bulk shipping industry.

both a fee and an exam. Moreover, taxis need to be equipped with a physical meter, which captures the number of kilometers traveled in the "occupied" mode and the billed amount. Meters need to be certified every two years by a state agency. Each meter records the aggregate numbers of kilometers billed together with the revenues. A licensed driver may find rides by searching for street-hail consumers or by choosing to participate in a dispatch service. Among dispatch options are traditional telephone-based dispatch services and, more recently, the app-based ride-hail platform that we study. This regulatory environment is different from most US municipalities, in which there is nearly free entry into the ride-hail market through firms such as Uber and Lyft. In the period that we study, Liftago is by far the dominant platform in Prague.[9]

Drivers pay a percentage fee for each ride that is booked through the platform. By tracking both the taxi's GPS and the time of the trip, it provides an approximate fare before the trip begins and a final fare after its completion. Because Liftago is not well known internationally, few riders are tourists, making our estimates easier to interpret in terms of local economic quantities.[10]

Drivers and consumers are matched by a combination of a dispatch algorithm and an auction. Whenever a consumer requests a ride, the system looks for nearby available cars and sends requests to a certain number of them, typically four, to elicit an offer. A driver who receives a request observes the details of the trip — the location of the consumer, the destination, consumer rating, and payment via cash or credit. A driver who is interested in fulfilling the ride submits a bid from a set of pre-programmed tariffs.[11] A tariff consists of a flag fee, a per-minute waiting fee, and a per-kilometer fee with a regulatory cap at CZK 36 ($\approx$ \$1.41). The platform takes tariff bids and combines them with a query to Waze, a real-time traffic mapping service and Google subsidiary, which provides estimates of the taxi arrival time (equivalently, the consumer *waiting time*), the trip time, and trip distance. The tariff bids are then translated into a single expected price for a trip. The consumer then observes bids as final trip prices together with other bid-specific attributes: the waiting time until the taxi arrives, the make and model of the car, and the driver's rating. Importantly, these non-price attributes are automatically attached to each of the bids; in each auction, drivers only have control over the tariff. The consumer may select one of the bids, in which case the ride occurs, or may decline all bids. When the ride is completed, the consumer pays the fare shown on the meter.[12] Figure A.1 in Appendix A shows the interface that riders see on the app before the request and after the request arrives.

A noteworthy consequence of Liftago's mechanism is that it allows for variation in both

[9]Uber has also been present in Prague since 2014, but its presence is not as large as in a typical US city of similar size, partially since it is still fighting several legal battles due to various licensing and taxation issues. Since an EU court's decision in December 2017, Uber is viewed as a transportation company and hence its drivers also need to be properly licensed.

[10]This is also reflected in the relatively small fraction of airport rides, which comprise about 2% of total trips.

[11]Drivers who supply rides in Liftago typically have a large number of pre-programmed bid increments.

[12]The app and an email receipt from Liftago only display an estimated amount. However, if the actual amount differs from the estimated amount, consumers are encouraged to report the discrepancy. Drivers can be banned from the platform if they are found regularly overcharging.

prices and waiting times: a driver with a high waiting time may submit a lower bid than a driver with a low waiting time, and vice versa. Contrast this market clearing mechanism with traditional taxi services, where prices are fixed so that the market clears through adjustments in waiting time, and with other ride-hail platforms, where prices are adjusted to keep waiting times stable.

2.2 Data

Our dataset covers 1.9 million trip requests and 1.1 million actual trips on Liftago between September 30, 2016 and June 30, 2018. For each request, we observe the time of the request, the pick-up and drop-off location, trip price bids and estimated waiting times from each driver, and which bid the consumer chose, if any. In addition, we observe a unique identifier for each driver and consumer. The sample period includes 1,455 unique drivers and 113,916 unique consumers.

We complement the data for each ride request with geospatial and public transportation data from the Google Transit Matrix API, based on the GPS addresses for each origin and destination in the Liftago data. The API data provide us with alternative public transit times for each origin-destination pair. Furthermore, we use data on (i) hourly rainfall to attach prevailing weather characteristics, and (ii) GPS-specific land values from GIS coded data.[13]

Table 1 summarizes daily activity on the platform. About $3,000$ trip requests are made each day, 61% of which become rides. The average bid is \$10.72 and the average waiting time is 7 minutes. In addition, about one third of the drivers in the sample were active each day. The average number of drivers bidding in each auction is 2.8, and except in rare cases there are no more than four bids.[14]

[13] We obtain this information from https://www.noaa.gov/ and http://www.geoportalpraha.cz, respectively.

[14] We discard auctions with more than four bids, representing only 0.33% of the sample.

Table 1: Bid, Order, and Daily Summary Statistics

	Full Sample *N=1,872,362 orders*				Weekdays Only (M-F) *N=1,337,826 orders*			
Variable	**P25**	**Mean**	**P75**	**S.D.**	**P25**	**Mean**	**P75**	**S.D.**
PANEL A: CHOSEN TRIP SUMMARY (ACROSS-AUCTION)								
Price of Trip (USD)	6.16	9.31	11.23	4.63	6.13	9.24	11.11	4.58
Wait Time (minutes)	4.00	6.07	8.00	3.08	4.00	6.14	8.00	3.08
PANEL B: ALL BIDS SUMMARY (WITHIN-AUCTION)								
Price of Trip (USD)	9.95	10.72	11.47	1.17	9.79	10.57	11.31	1.16
Wait Time (minutes)	5.81	7.01	8.22	1.85	5.88	7.11	8.36	1.88
Number of Bids	2.00	2.79	4.00	1.09	2.00	2.81	4.00	1.08
PANEL C: DAILY SUMMARY (N = 638 *days*)								
Number of Requests/Day	2319	2934	3520	956	2376	2940	3486	947
Number Trips/Day	1410	1785	2149	557	1502	1831	2180	569
Number Drivers/Day	464	499	553	89	491	518	569	90

NOTE: Table 1 shows summary statistics at the auction level (Panel A), the bid level (Panel B) and the daily level (Panel C). P25 refers to the 25th percentile and P75 to the 75th percentile of the respective variable. Panel B reports the average over each statistic computed within each auction.

2.3 Preferences over Time and Money: Intra-daily Patterns

In this section we provide descriptive evidence for the spatial and inter-temporal patterns in prices, waiting times, and choices. We document large and interpretable heterogeneity in consumer choices, which provides important identifying variation for our model. Figure 1 shows the average trip price (Figure 1a) and wait times (Figure 1b) by day of the week and time of the day. Prices are lower during weekday afternoons and higher during weekends, while wait times tend to be substantially higher during the day compared with overnight hours.

Consumers in our data often face a non-trivial trade-off between price and waiting time when choosing among bids. A trade-off implies the existence of options such that one has a lower waiting time but a higher price and vice versa. Depending on the time of day, about 58%–70% of auctions involve a trade-off between waiting less and paying more (Figure B.1 in Appendix B provides additional detail).

Figure 2a shows how consumers solve the trade-off between time and monetary costs at different times of the day. At all times of day, consumers are more likely to pick the minimum price option than the minimum waiting-time option. The elasticities that we back out from our model are in line with this observation. Moreover, the magnitudes of these differences vary throughout the day. During work hours, there is a significant dip in the likelihood of choosing the lowest price option and an even larger increase in the likelihood of choosing the lowest

Figure 1: Prices and Waiting Times by Hour and Day

(a) Average Prices

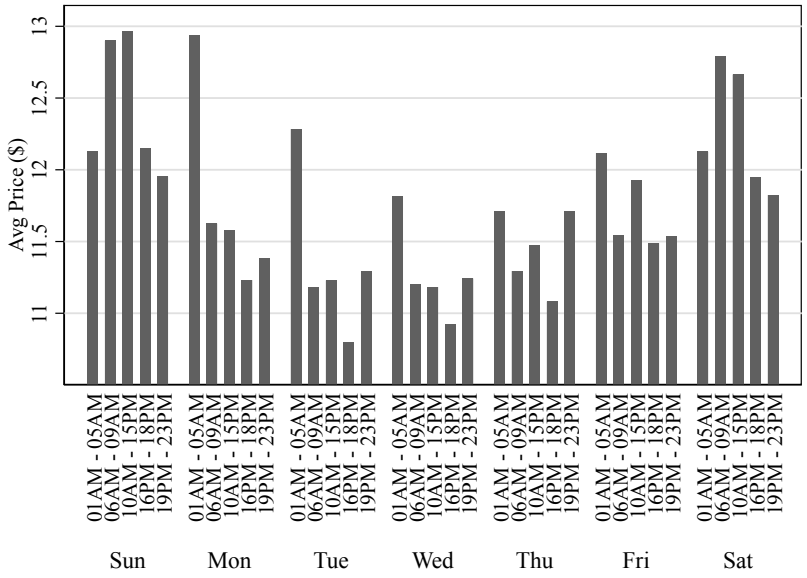

(b) Average Wait Times

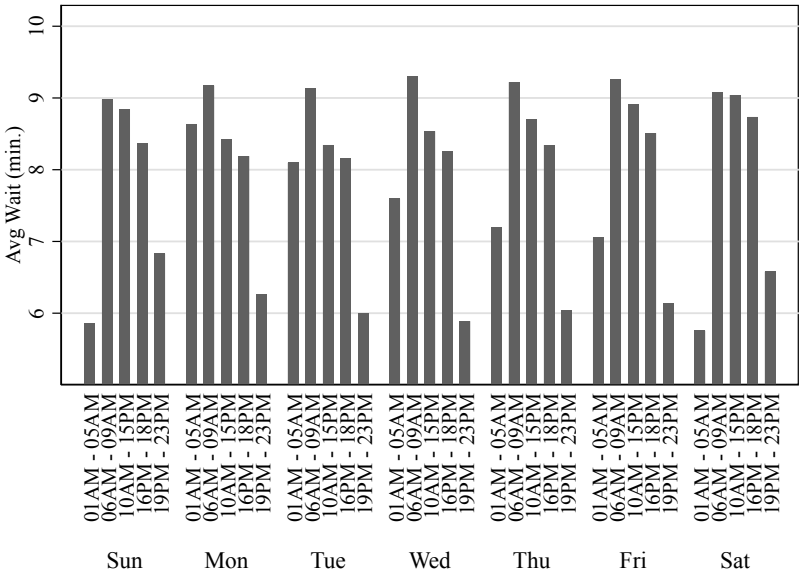

NOTE: Figure 1 shows the average offer prices (Figure 1a) and average waiting times (Figure 1b) across all bids submitted on different days of the week and at different times of day.

wait option.[15] This pattern can be attributed to some combination of preference heterogeneity across consumers as well as within-consumer heterogeneity throughout the day. Because we observe consumer identifiers, our model leverages the variation across consumers to identify

[15]Note those two do not have to add up to one because a consumer might, for example, choose a driver with the highest rating even if that driver neither offers the lowest price nor provides the lowest wait time.

individual-level preference heterogeneity.

We next show how choices differ by location. To partition Prague into smaller regions, we use a data-driven approach by clustering GPS locations of trip origins and destinations. We use a *k-means* procedure with the number of locations set to 30, which balances the richness of spatial preference heterogeneity and sample size. The resulting map is shown in Figure A.2 in Appendix A.

Figure 2b compares choices over price and wait times by pickup location. Within each pickup location, Figure 2b shows the probability that consumers choose the lowest price and/or wait time among all available bids, computed only within auctions that feature a tradeoff between prices and waiting times. Locations are sorted by the probability of choosing the lowest price. Like Figure 2a, Figure 2b demonstrates that consumers exhibit preferences for lower prices and waiting times. It shows that minimum prices are chosen about two to three times more often than minimum waiting times, but heterogeneity also exists across locations. Although situational factors might play an important role in consumers' decisions to make a trip, Figure 2b indicates that there are long-run differences in preferences over waiting times across locations.

Figure 2: Trade-offs and choices

(a) By Hour

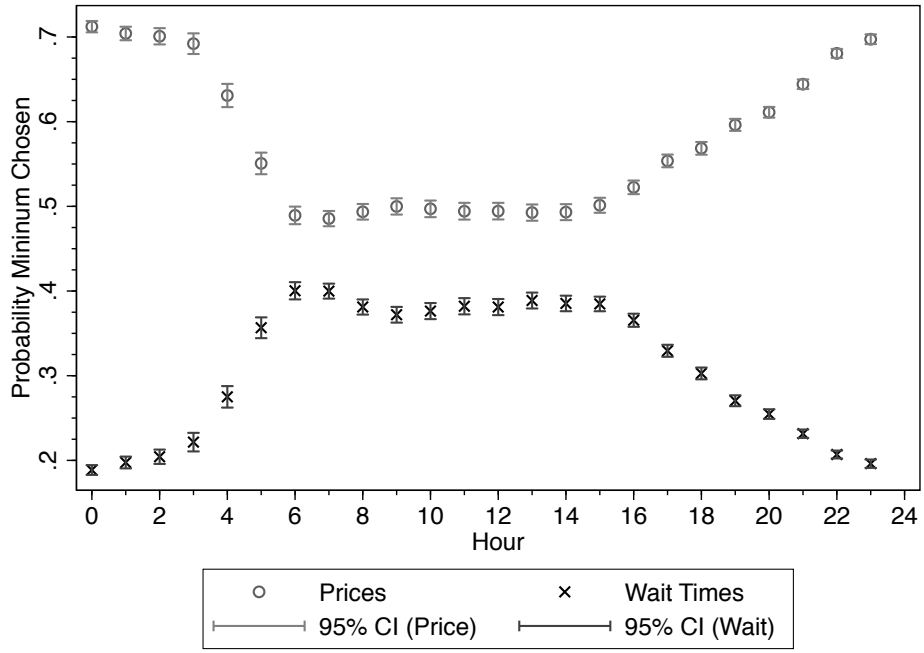

(b) By Pickup Location

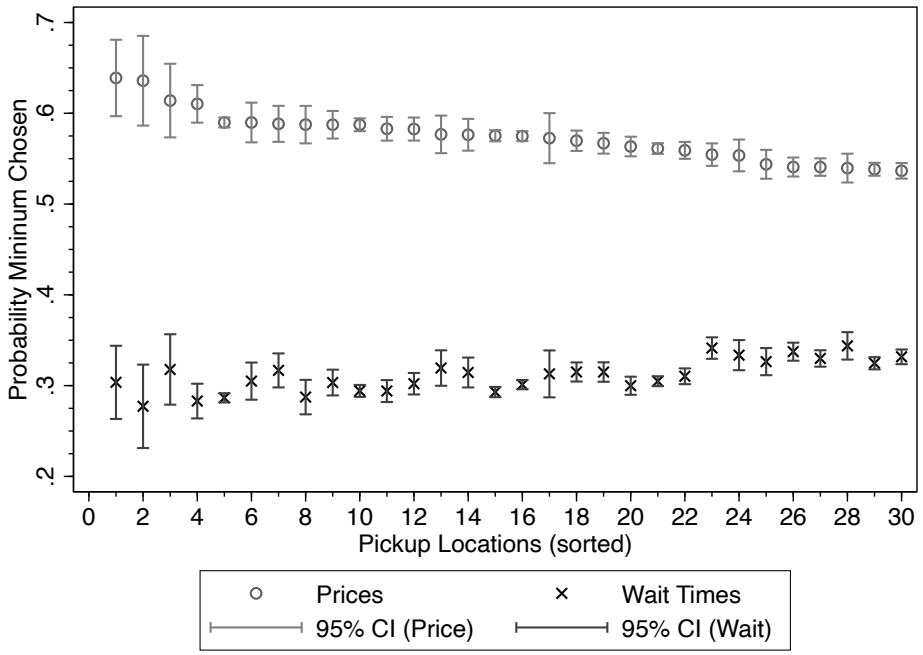

NOTE: Figure 2 shows the mean probability that a consumer who faces a trade-off between price and waiting time chooses either the lowest price or lowest waiting time. Probabilities are computed among orders in which one of the bids was chosen over the outside option. Probabilities are computed among orders in which one of the bids was chosen over the outside option. In Figure 2b, locations are sorted by the probability of choosing the lowest price.

3 Demand

Section 3 describes the demand side of the platform. Section 3.1 describes the conceptual framework that we use to relate a consumer's choice between two trips to her value of time. Section 3.2 then describes the discrete choice model of demand that we estimate and how it maps to the framework in Section 3.1. Finally, Section 3.3 describes the empirical strategy.

3.1 Interpretation of Choices among Orders

We now describe the trade-off choices on the platform entail. We do so through a model of consumer choice in the spirit of Small (1982), Fosgerau et al. (2007), and Tseng and Verhoef (2008), among others. After introducing the model and our definition of the value of time (see Equation 2 below), we contrast our definition with that usually considered in the transportation literature.

We describe a consumer by a pair of valuations $(v^O, v^D) : [0, T] \mapsto \mathbb{R}^2$, which denote their utility from spending time t at either the origin, O, or the destination, D. This specification assumes that the value of the time spent on the ride is 0. Alternatively, this means that v^O represents the value of spending time at the origin, net of the value of the time spent traveling, whereas v^D represents the value of spending time at the destination, net of value of the time spent traveling. Further, these functions will depend on the locations $a \in \mathcal{A}$ of the origin and the destination, which we denote by $v^O_a, v^D_{\hat{a}}$ if location a is the origin and $\hat{a}$ is the destination. Finally, we assume the consumer has linear preferences in money.

Given the above primitives, we can derive the consumer's utility from taking a given trip. For illustration, suppose the consumer starts at time $t = 0$ at origin O and requests a ride at time t_r to go to destination D. Moving from the origin to the destination involves some travel time, Δ, and the time waiting for the ride, w. If the consumer asks for a ride at $t_r \geq 0$ with an estimated time of arrival of w and a price of b, her utility is given by

$$u(t_r, w, b) = \int_0^{t_r+w} v^O(t)dt + \int_{t_r+w+\Delta}^{T} v^D(t)dt - b. \tag{1}$$

Now, on our platform, the consumer chooses between different trips, which have different prices and wait times. Figure 3 illustrates how the choice of which trip to accept affects the time allocation between the origin and the destination. Suppose that when the consumer requests a ride, she receives two bids. Because both drivers are supposed to take the same optimal route, the time from the pickup to the destination is the same and given by Δ. The two trips differ in the drivers' estimated time of arrival. The second trip leads to a longer wait time w_2. By accepting the first trip, the consumer decides to spend $w_2 - w_1$ less time at the origin and $w_2 - w_1$ more time at the destination.

Figure 3: Origin Destination Trade-Off in Waiting-Time Choice

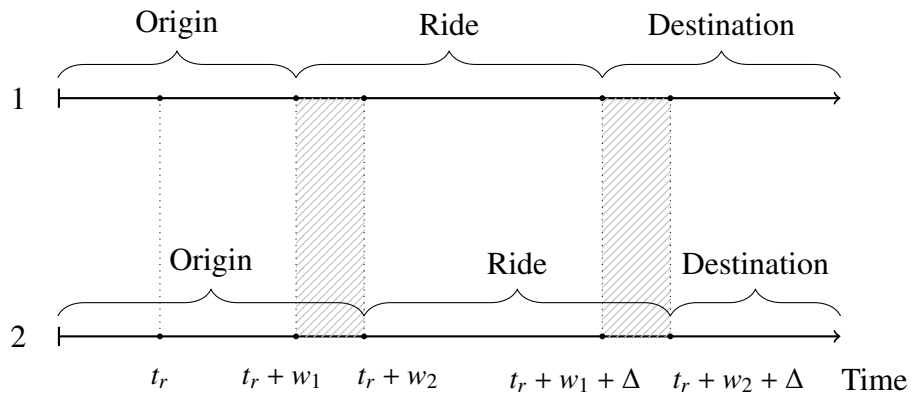

NOTE: Figure 3 depicts the trade-off between two hypothetical trip options beginning with request time t_r and constant travel time Δ. Trip option has wait time w_1 and arrival time $t_r + w_1 + \Delta$. Trip option two has wait time w_2 and arrival time $t_r + w_2 + \Delta$.

Let a and $\hat{a}$ denote the origin and destination, respectively. When considering the two trip options, the consumer compares $v_a^O \cdot (w_2 - w_1)$ with $v_{\hat{a}}^D \cdot (w_2 - w_1)$, up to an approximation. Letting the difference between w_2 and w_1 be one unit (e.g., 1 minute), the willingness to pay for waiting-time reductions, which we call the *value of time*, can be expressed as

$$\text{VOT}_{a \to \hat{a}} = v_{\hat{a}}^D - v_a^O. \tag{2}$$

Note that whereas in the transportation literature (e.g., Small, 1982), the value of time refers to the value of travel-time savings, we define the value of time as the difference between the value of being at the origin and the destination. Our model therefore focuses on the implicit trade-off over locations that is implied by different wait-times, holding time in the car fixed.

3.2 Model of Travel Choice

Whereas Section 3.1 treats $\text{VOT}_{a \to \hat{a}}$ as directly observed, we describe in this section how to recover $\text{VOT}_{a \to \hat{a}}$ from a standard discrete choice framework that models indirect utilities over trips. The set of consumers is indexed by $i \in \{1, \ldots, I\}$ and the set of locations is indexed by $a \in \{1, ..., A\}$. Time is indexed by $t \in \{1, \ldots, T\}$. Furthermore, we consider a coarser partition of time, indexed by $h \in \{1, \ldots, H\}$, which allows us to signify that some variables vary across different hours, but perhaps not across different minutes, of the day.

When presented with a menu of bids (or offers) for a ride between a and $\hat{a}$ in period t, the consumer makes a discrete choice between J options. Each alternative $j \in \{1, \ldots, J\}$ is characterized by a tuple consisting of price, wait time, route characteristics such as distance, characteristics of the car (model, year, color), driver (ratings and name), and a stochastic part

$\epsilon_{i,j,t}$. We capture observable trip differences with $\mathbf{x}_{i,j,t}$. We also have to account for an additional term, $\xi_{a,\hat{a},t}$, that captures unobserved conditions affecting demand on a particular route, such as large sporting events or transit delays. We discuss endogeneity concerns in Section 3.3.

With this setup, the indirect utility from option j can be written as

$$\begin{aligned} u_{i,j,t}(w_{j,t}, b_{j,t}, \mathbf{x}_{i,j,h}, \epsilon_{i,j,t}; \boldsymbol{\beta}) &= \beta^{w}_{i,h_t,a,\hat{a}} \cdot w_{j,t} + \beta^{p}_{i,h_t} \cdot b_{j,t} + \beta^{x} \cdot \mathbf{x}_{i,j,t} + \xi_{a,\hat{a},t} + \epsilon_{i,j,t} \\ &= \overline{u}_{i,j,t}(w_{j,t}, b_{j,t}, \mathbf{x}_{i,j,t}; \boldsymbol{\beta}) + \epsilon_{i,j,t}, \end{aligned} \tag{3}$$

where β^{p}_{i,h_t} and $\beta^{w}_{i,h_t,a,\hat{a}}$ reflect preferences over price and waiting time, and the subscripts h_t, a, and $\hat{a}$ in $\beta^{w}_{\cdot}$ indicate that we allow preferences over waiting time to vary with the hour of the day as well as by origin and destination.[16] The coefficient β^{x} captures preferences for other bid-specific characteristics (distance, driver's rating, car type, etc.) as well as environmental conditions common to all drivers j: hour of day, public transit availability, traffic speeds, trip distance and time, rainfall, origin and destination neighborhoods, and whether the order is placed on the street or in a building.

We specify h_t as follows: the price coefficient is allowed to vary between work hours (defined to be 9am–6pm) and non-work hours. The waiting-time coefficient is allowed to vary across five blocks of time. The omitted category is the midnight hour, 12am to 1am. The remaining blocks are 1am to 5am, 6am to 9am, 10am to 3pm, 4pm to 6pm, and 7pm to 12am. We also control for drivers' quality ratings, car type, traffic speed and trip distance.

We can then map the preference parameters in Equation 3 into VOT's for different locations and different times of day. These VOT's are obtained via the following equality, which compares the utility of choice j with the utility of some hypothetical option j' that adds a single minute to the waiting time, but otherwise has the same characteristics. The difference $b_{j,t} - b_{j',t}$ that solves the equation reflects the additional units of money needed to make consumers, on average, indifferent between paying or waiting more:

$$\beta^{p}_{i,h_t} \cdot b_{j,t} + \beta^{w}_{i,h_t,a,\hat{a}} \cdot w_{j,t} = \beta^{p}_{i,h_t} \cdot b_{j',t} + \beta^{w}_{i,h_t,a,\hat{a}} \cdot (w_{j,t} + 1). \tag{4}$$

This implies a minute of time at destination $\hat{a}$ relative to its value at origin a is valued as

$$\text{VOT}_{a \to \hat{a},h_t,i} = b_{j,t} - b_{j',t} = \frac{\beta^{w}_{i,h_t,a,\hat{a}}}{\beta^{p}_{i,h_t}}. \tag{5}$$

Equation 5 demonstrates that individual estimates of the value of time can be recovered directly from the estimated demand model by taking a ratio of coefficients.

[16] Our specification also includes a utility parameter on the square of the waiting time, which we omit from Equation 3 for expositional clarity. As we discuss in Section 5.1, the parameter estimate is small and therefore does not play a major role in the analysis.

3.3 Demand Estimation

This section discusses the details of our estimation procedure, which proceeds as follows. We estimate a likelihood model based on the individual choices over bids on the app. To capture time- and location-specific heterogeneity in time values, we interact all waiting-time parameters with time-of-day fixed effects, and include separate fixed effects for each origin and destination. To capture individual-specific heterogeneity, we leverage the panel structure of our data to compute random coefficients on both price and waiting time using an MCMC procedure. To allow for better interpretation of this heterogeneity, the analysis hereafter only utilizes weekday data.

Mixed Logit Discrete Choice Model Under the assumption that $\epsilon_{i,j,t}$ are independently and identically distributed according to a Type I extreme value distribution, choosing the maximum among J alternatives with utilities given by Equation 3 reduces to the standard logit. The probability that an alternative j is chosen depends on its relative mean utility and is given by

$$l(w_{j,t}, b_{j,t}, \mathbf{x}_{i,j,t}; \boldsymbol{\beta}) = \frac{\exp(\beta^w_{i,h_t,a,\hat{a}} \cdot w_{j,t} + \beta^p_{i,h_t} \cdot b_{j,t} + \beta^x \cdot \mathbf{x}_{i,j,t})}{\exp(-\xi_{a,\hat{a},t}) + \sum_k \exp(\beta^w_{i,h_t,a,\hat{a}} \cdot w_{k,t} + \beta^p_{i,h_t} \cdot b_{k,t} + \beta^x \cdot \mathbf{x}_{i,k,t})}. \tag{6}$$

For bid-specific attributes we, as the econometricians, are on almost equal footing with consumers, because we observe all relevant bid attributes up to the drivers' names and photos. These unobserved features are therefore part of $\epsilon_{i,j,t}$.

However, because drivers might condition their bids on unobserved conditions $\xi_{a,\hat{a},t}$, bids could still be correlated with unobservable demand conditions and thereby bias the price coefficients. To deal with this concern, we leverage persistent differences in bids among different drivers.[17] These differences might, for example, arise from pre-programmed bid increments in the meter. Because our model relies on individual choice data and is likelihood based, we cannot use standard inversion techniques to isolate $\xi_{a,\hat{a},t}$ and directly instrument. To get around this issue, we concentrate $\xi_{a,\hat{a},t}$ out using a control function approach (Petrin and Train, 2010). This step consists of a simple regression of trip prices on a set of driver fixed effects, from which we recover a residual that enters the likelihood as a control.[18]

The consumer's outside option is to reject all of the bids in a given order. We allow the value of outside option to vary at the level of each specific order in the data. We control for origin and destination locations, hourly rainfall, and whether the trip was ordered from within a building

[17] This approach is similar to a literature that exploits different leniency standards of judges, known as the *judge design*. See, e.g., Waldfogel (1995).

[18] Appendix B.5 provides further details on our control function approach. Figure B.5 in Appendix B.5.1 shows the resulting distribution of fixed effects, which demonstrates large and persistent variation in driver bids. The interquartile range is \$1.90, or 20% of the average fare, and the range from the 10th to the 90th percentile is \$4.00, or 43% of the average fare. Appendix B.5.2 shows that without the control function we find smaller price and waiting-time elasticities, resulting in an overall mean VOT that is 19% lower.

or outside on the street. We also incorporate detailed public transit data including the time-of-day-specific availability of public transit within walking distance between each individual order's origin and destinations points. These characteristics impact the value of the outside option available to consumers. We normalize the value of the outside option to zero during 12 am and 1am at a location without any nearby public transit option, when it is not raining, and when the order is placed inside a building. Note this specification allows for spatial (across different origin-destination pairs) and time-of-day variation in the outside option.

Our estimation exploits the panel structure of our data to capture the full heterogeneity in consumer preferences in a tractable way. In particular, we opt for a hierarchical Bayes mixed-logit model to obtain individual-specific estimates for the disutilities of both waiting and money. We use an MCMC method using data augmentation of latent variables as in Tanner and Wong (1987). In this approach, the unobserved random coefficients are simulated and then these simulations are treated as data. This method sidesteps the need to evaluate multidimensional integrals by instead sampling from a truncated Normal distribution. Following techniques described in Rossi and Allenby (2003), Rossi et al. (2005), and Train (2009), we now explain the particular version of the Gibbs sampler that we construct.

We assume individual waiting-time coefficients are additive in time of day, location, and an individual-specific shifter:

$$\beta^w_{i,h_t,a,\hat{a}} = \beta^w_i + \beta^w_a + \beta^w_{\hat{a}} + \beta^w_{h_t}. \tag{7}$$

Instead, consistent with the fungibility of money we allow for only minimal variation in price coefficients within an individual consumer. They are additive in an individual-specific and a time-of-day specific shifter:[19]

$$\beta^p_{i,h_t} = \beta^p_i + \beta^p_{h_t}. \tag{8}$$

We assume that the individual-specific shifters are normally distributed. Formally, $\boldsymbol{\beta}_i \sim \mathcal{N}(\boldsymbol{\mu}, \boldsymbol{\Sigma})$, where $\boldsymbol{\beta}_i \equiv (\beta^w_i, \beta^p_i)$, is the vector of coefficients that vary at the individual level. The matrix $\boldsymbol{\Sigma}$ denotes the variance of the individual-specific components of the coefficients as well as their covariance. The covariance $\sigma_{w,p}$ tells us whether people who are more elastic to waiting times are also more elastic to price. We would expect a positive covariance since the utility of income should be related to the opportunity cost of time. However, one can also imagine segments of the population who are wealthy and yet have an abundance of disposable

[19]The rationale for allowing the price coefficients to vary during day and night hours is to capture the possibility that daytime business trips are reimbursed.

time, such as rich retirees.

$$\mathbf{\Sigma} = \begin{pmatrix} \sigma_w & \sigma_{w,p} \\ \sigma_{w,p} & \sigma_p \end{pmatrix}. \tag{9}$$

We assume $\boldsymbol{\mu} \sim \mathcal{N}(\mu_0, \Sigma_0)$, where Σ_0 is a diffuse prior (unboundedly large variance). We assume the hyper-parameters of the variance are Inverse-Wishart, $\Sigma_0 \sim IW(v_0, S_0)$. One can then iteratively update the coefficient vector, $\boldsymbol{\beta}_i$, the mean of the coefficients, as well as their standard deviations. The specific assumptions we make about the priors lead to conjugate distributions where the posterior mean of $\boldsymbol{\beta}_i$ is itself normal and the variance is again in the family of inverse gamma distributions. To describe the updating algorithm, let $\overline{\boldsymbol{\mu}}^l$ be the sample mean of coefficients of iteration l in the chain, and let S^l be the sample variance of the Inverse-Wishart.

The key simplification exploited in the Gibbs sampler is that one does not have to obtain an analytical expression for the posterior distribution of the $\boldsymbol{\beta}_i$'s, which instead only requires a proportionality factor that can be easily computed at each step. In particular, we have

$$K(\beta_i \mid \boldsymbol{\mu}^l, \mathbf{\Sigma}^l, \mathbf{y}_i) \propto \prod_{t=1}^{T_i} l(w_{j,t}, b_{j,t}, \mathbf{x}_{i,j,t}; \boldsymbol{\beta}) \cdot \phi(\boldsymbol{\beta}_i \mid \boldsymbol{\mu}^l, \mathbf{\Sigma}^l), \tag{10}$$

where $\mathbf{y}_i$ is the vector of choices and covariates observed for consumer i with T_i observations and $l(\cdot; \boldsymbol{\beta}_i)$ is the likelihood contribution of a particular choice. The iterative updating is then given by the following steps:

1. Draw a new posterior mean $\boldsymbol{\mu}^l$ for the distribution of coefficients from $\mathcal{N}(\overline{\boldsymbol{\mu}}^{l-1}, \frac{W}{N})$.
2. Draw $\mathbf{\Sigma}^l$ from $IW(K+N, S^l)$, where $S^l = \frac{K \cdot I + N \cdot S_1^l}{K+N}$ and $S_1^l = \frac{1}{N} \cdot \sum_i^N (\boldsymbol{\beta}_i^{l-1} - \overline{\boldsymbol{\mu}}^{l-1}) \cdot (\boldsymbol{\beta}_i^{l-1} - \overline{\boldsymbol{\mu}}^{l-1})'$.
3. For each i, draw $\boldsymbol{\beta}_i^l$ according to the Metropolis Hastings algorithm, with new proposal $\boldsymbol{\beta}_i^{pl}$ starting from $\boldsymbol{\beta}_i^{l-1}$ using density $\phi(\boldsymbol{\beta}_i | \boldsymbol{\mu}^l, \mathbf{\Sigma}^l)$.

Such an MCMC procedure is known to be slow for a large-dimensional parameter space. To avoid slow convergence we first estimate the model without the random coefficients using standard maximum likelihood and then employ the Gibbs sampler to obtain the distribution of random coefficients separately, starting from the maximum likelihood estimates.

4 Supply

Section 4 introduces the supply side of the platform. Section 4.1 presents the model of driver bidding on the platform. Section 4.2 explains how we estimate the model and shows how we

can link a driver's bid, which we observe, to their opportunity cost of serving a ride, which we do not observe. We show how drivers' dynamic optimization problem can be recast as a static auction, which allows us to recover opportunity costs in a form that is sufficient for the pricing counterfactuals that we consider in Section 6.

4.1 Model of Driver Bidding

Our model of driver bidding captures the following trade-off: when a driver receives a ride request on the platform and successfully bids for it, the driver gives up on the value of remaining idle at a given location. This value consists of two parts. First, there is the immediate value of staying at that location, such as the opportunity to immediately serve a different ride on the taxi market. Below, we refer to this component as the driver's *outside option*, which is period specific. Second, there is the continuation value of staying at that location. The driver may prefer to wait to serve a more profitable ride on either the platform or the taxi market. Thus, when deciding whether and how much to bid for a ride, the driver compares the value of the ride with the value of remaining idle on the platform at a given location and point in time.

More formally, in each period t and each location a, timing is as follows. First, each driver j available in period t at a observes the value of their outside option, $\kappa_{j,t}$, which describes the value of not serving a trip on the platform in that period and that location. The outside option $\kappa_{j,t}$ is drawn from a possibly time- and location-dependent distribution, $G_t(\cdot|a)$. Second, each driver either receives a request from the platform ($\rho = 1$) or not ($\rho = 0$). Note that from the perspective of the driver, this is a random (and potentially location- and time-dependent) event, so that below we abuse notation and let $\rho_t(a)$ denote the total probability that the driver receives a request from the platform at location a in period t. For simplicity, below we suppress the dependence of ρ on (t, a). A driver who receives no requests from the platform earns the outside option $\kappa_{j,t}$. Instead, a driver who receives a request from the platform observes the trip's characteristics, such as the estimated time to arrival and the destination, and submits a bid for that trip simultaneously with the other drivers that received the same request. If the consumer selects driver j, driver j serves the ride. Instead, if the rider does not select driver j, the driver earns the outside option $\kappa_{j,t}$. At the end of period t, drivers transition out of a only if they win the auction. No independent location choice is made.

Driver j's state in period t then consists of the value of the outside option $\kappa_{j,t}$ and the location a. Thus, driver j's value at state $(\kappa_{j,t}, a)$, $\mathcal{S}_{j,t}(\kappa_{j,t}, a)$, is given by[20]

$$\mathcal{S}_{j,t}(\kappa_{j,t}, a) = (1-\rho) \cdot \left[\kappa_{j,t} + \delta \cdot \mathbb{E}_{G_{t+1}(\cdot|a)}[\mathcal{S}_{j,t+1}(\cdot, a)]\right] + \rho \cdot \mathbb{E}_{\mathbf{z}}[\mathcal{V}_{j,t}(\kappa_{j,t}, a, \cdot)]. \tag{11}$$

[20] Implicit in our formulation is the assumption that a driver's bidding behavior does not depend on how they arrived at location a in period t: Besides their individual characteristics (e.g., car make, rating), only the current time period, location, and outside option realization matter to determine their bidding behavior.

In words, a driver that does not receive a request collects their outside option, $\kappa_{j,t}$, and earns the continuation value of remaining at location a in period $t+1$. Otherwise, a driver gets a ride request and obtains the value of participating in the auction, denoted by $\mathcal{V}_{j,t}(\cdot)$. The value of participating in the auction depends on the driver's state $(\kappa_{j,t}, a)$ as well as on the characteristics of the trip they bid for, denoted by $\mathbf{z}_j$ — driver j's exogenous quality characteristics. These characteristics include the trip's observable characteristics $\mathbf{x}$, such as the consumer's destination, $\hat{a}$, together with the realized time to pick up the consumer, w.

We now unpack the value $\mathcal{V}_{j,t}$ of receiving a request from the platform. Suppose driver j receives a request for a trip described by $\mathbf{z}_j$, with time to pick up $w_{j,t}$, trip length Δ, and headed to location $\hat{a}$. Letting $\tau = w_{j,t} + \Delta$, if driver j wins the auction, they will be at location $\hat{a}$ in τ periods from now. Thus, we can write the driver's payoff from bidding for this trip as follows:

$$\mathcal{V}_{j,t}(\kappa_{j,t}, a, \mathbf{z}_j) = \max_b \Big\{ \gamma(b|a, \mathbf{z}_j) \cdot \Big(0.9 \cdot b + \delta^\tau \cdot \mathbb{E}_{G_{t+\tau}(\cdot|\hat{a})} \left[\mathcal{S}_{j,t+\tau}(\cdot, \hat{a}) \right] \Big) + (1 - \gamma(b|a, \mathbf{z}_j)) \cdot \Big(\kappa_{j,t} + \delta \cdot \mathbb{E}_{G_{t+1}(\cdot|a)} [\mathcal{S}_{j,t+1}(\cdot, a)] \Big) \Big\} \quad (12)$$

In words, upon receiving a request, the drivers essentially participate in an asymmetric first-price auction, where they compete on the price b under exogenous quality characteristics. With probability $\gamma(b|a, \mathbf{z}_j)$ – we unpack this probability below– driver j wins the auction, serves the ride at a price b, pays Liftago 10% of the trip's final price, and transitions to a new location in τ periods, where τ takes into account the wait time and the trip length. With probability $1 - \gamma(b|a, \mathbf{z}_j)$, the driver loses the auction and obtains the outside option and the opportunity to serve a trip in that location in period $t+1$. We do not separately model a driver's choice to reject a request because drivers can always submit a very high bid.

The probability of winning the auction, $\gamma(b|a, \mathbf{z}_j)$, is determined by the consumer's preferences over price and wait time, as well as other characteristics of the options in the consumer's choice set. Drivers do not observe anything about the other bidders when submitting their bid. The bids and quality attributes of other drivers, summarized by $\mathbf{z}_{-j} = (\mathbf{x}_{-j}, w_{-j})$, and the idiosyncratic components of consumer utility are therefore all stochastic from the perspective of driver j when submitting the bid. Under rational expectations about the distribution of the number of rivals, rivals' bids and wait times, and the consumer's preferences (Equation 3), driver j's probability of winning is given by

$$\gamma(b|a, \mathbf{z}_j) = \sum_{n=0}^{3} \lambda_n \cdot \left[\int \mathbb{P}\Big[u(b, w_{j,t}, \mathbf{x}_{j,t}; \boldsymbol{\beta}_i) \geq \max_{k \in \{0,\dots,n\}} u(b_k, w_{k,t}, \mathbf{x}_{k,t}; \boldsymbol{\beta}_i) \Big] \, dF_n(\mathbf{b}_{-j}, \mathbf{z}_{-j}|a) d\Phi(\boldsymbol{\beta}_i) \right], \quad (13)$$

where (i) λ_n denotes the probability that driver j faces n other competing drivers, (ii) $\mathbf{b}_{-j}$ and $\mathbf{z}_{-j}$ denote the vectors of rivals' bids and attributes respectively, (iii) F_{-n} is the distribution of other drivers' bids and characteristics, and (iv) $d\Phi(\boldsymbol{\beta}_i)$ signifies that at the moment of submitting a

bid, driver j also faces uncertainty over the consumer's preferences.[21]

4.2 Driver Costs: Identification and Estimation Details

The supply-side estimation consists of the following. We first show that the dynamic program (Equation 12) can be mapped into a static auction, as in Jofre-Bonet and Pesendorfer (2003). Given our demand estimates, we show that we can use techniques similar to those in Guerre et al. (2000) to back out the *pseudo-costs* that rationalize the observed bids. These pseudo-costs include all of the components that factor into a driver's decision to submit a bid, including the difference in continuation values. Note we can rewrite the maximization problem in Equation 12 in a way that directly maps into a static auction setup:

$$\begin{aligned}\mathcal{V}_{j,t}(\kappa_{j,t}, a, \mathbf{z}_j) = \max_b \Big\{ & \kappa_{j,t} + \delta \cdot \mathbb{E}_{G_{t+1}(\cdot|a)}[\mathcal{S}_{j,t+1}(\cdot, a)] + \\ & \gamma(b|a, \mathbf{z}_j) \cdot \Big(0.9 \cdot b + \delta^\tau \cdot \mathbb{E}_{G_{t+\tau}(\cdot|\hat{a})}[\mathcal{S}_{j,t+\tau}(\cdot, \hat{a})] - \kappa_{j,t} - \delta \mathbb{E}_{G_{t+1}(\cdot|a)}[\mathcal{S}_{j,t+1}(\cdot, a)]\Big)\Big\} \end{aligned} \tag{14}$$

We can define the pseudo-cost that entails both the per-period opportunity cost as well as any differences in continuation values that arise from accepting a bid:

$$\begin{aligned} c_{j,t}^{t+\tau}\left(a, \hat{a}, \kappa_{j,t}\right) &\equiv \kappa_{j,t} + \delta \cdot \mathbb{E}_{G_{t+1}(\cdot|a)}[\mathcal{S}_{j,t}(\kappa_{t+1}, a)] - \delta^\tau \cdot \mathbb{E}_{G_{t+\tau}(\cdot|\hat{a})}\left[\mathcal{S}_{j,t+1}(\kappa_{t+\tau}, \hat{a})\right] \\ &= \kappa_{j,t} + e_{j,t}^{t+\tau}(a, \hat{a}), \end{aligned} \tag{15}$$

where the notation e represents the *endogenous* part of the drivers' pseudo-costs. Note, however, that e is actually a *convex* combination of exogenous costs (future realizations of the outside option) and endogenous costs (future bids for trips served on the platform). Since queries on the platform are not very frequent, it is safe to assume that e is almost invariant to changes within the platform. Therefore, when considering drivers' bid re-optimization, as we do in our counterfactual analysis, it is enough to know drivers' pseudo-costs.

Proposition 1. *The distribution of pseudo-costs is non-parametrically identified from drivers' bids and the demand model estimates.*

Proof of Proposition 1. We can rewrite the driver's problem as

$$\max_b \gamma(b|a, \mathbf{z}_j) \cdot \left(0.9 \cdot b - c_{j,t}^{t+\tau}(a, \hat{a}_{t+\tau}, \kappa_{j,t})\right). \tag{16}$$

[21] Recall that β is normally distributed (see Section 3.3).

From first order conditions we get[22]

$$c_{j,t}^{t+\tau}\left(a, \hat{a}, \kappa_{j,t}\right) = 0.9 \cdot \left(b + \frac{\gamma(b|a, \mathbf{z}_j)}{\gamma'(b|a, \mathbf{z}_j)}\right). \tag{17}$$

The bid on the right-hand side is directly observed. Moreover, with estimates from the demand system we can compute $\hat{\gamma}(b|a, \mathbf{z}_j)$ and $\hat{\gamma}'(b|a, \mathbf{z}_j)$, building on Equation 13, so that all the objects on the left-hand side are observed. □

Because the proof of Proposition 1 is constructive, we can simply back out the driver's cost bid by bid, using Equation 17. However, for each order we only observe one realization of competing bids. To compute $\gamma(\cdot|a, \mathbf{z}_j)$, which includes drivers' time- and location-dependent expectations about competitors and consumers, we sample from the observed distribution of bids and consumers (Hortaçsu and McAdams, 2010). For each bid observed in the data, we simulate $s = 50$ requests. For each request, we draw a consumer preference vector $\boldsymbol{\beta}_i$ and a set of competing drivers according to $\hat{\lambda}_n$. To simulate the correct conditional expectation, the bids and attributes of competing drivers are drawn conditional on location a and time of day t as well as the length of the trip. With these simulation draws, we can construct the sample analogue $\hat{\gamma}(\cdot|a, \mathbf{z}_j)$ and $\hat{\gamma}'(\cdot|a, \mathbf{z}_j)$.

From pseudo-costs to $\kappa_{j,t}$ and $e_{j,t}$ We show in Appendix C.1 that the entire driver supply side model is identified. Once we have recovered the pseudo cost $c(\cdot)$, we can further decompose it into its primitive component $\kappa_{j,t}$ and the parts that give rise to the endogenous component $e(\cdot)$. We show in Proposition 2 in Appendix C.1 that $\kappa_{j,t}$ and all place- and time-dependent expectations that give rise to $c(\cdot)$ are separately identified. Moreover, our constructive proof shows that all driver primitives can be recovered through a simple regression of the pseudo-costs on a set of time- and location-specific dummies.

5 Results

We first present the results from the logit-demand model and the implied elasticities for both waiting time and price. We then show the value of time results implied by the demand estimates. Lastly, we present results on the opportunity costs of drivers.

5.1 Logit Model Results

Table 2 shows the coefficients and standard errors that we obtain from the demand model. Within an individual, we find that the price coefficient varies minimally across working and

[22] We assume a connected bid space. This is an approximation because drivers in reality bid in small increments of several cents.

non-working hours. The intra-daily coefficients on waiting time vary over time of day, increasing in absolute magnitude (becoming more negative) into the mid-day peak and declining into the evening. We find that the coefficient on waiting time squared is close to 0, which is consistent with what we see in the data: Figure B.2 in Appendix B.1 shows that the likelihood of picking a particular trip is close to a linear function of the waiting time and of the minimum wait time. The other two bid-specific attributes – driver rating and car type – are estimated to have a small but significant effect on utility; intuitively, consumers prefer drivers with higher ratings and better cars.[23] In addition, we also find variation in origin- and destination-specific heterogeneity in utility. Due to the large number of coefficients, we summarize the full set of location- and time-of-day-specific estimates separately in Figure B.3 and Figure B.4. These figures reflect that the vast majority of preference heterogeneity in waiting time and price is due to individual differences as opposed to location- or time-of-day-specific factors.

Our model captures rich substitution patterns dependent on driver-specific and environmental factors. The outside option is chosen about 33% of the time. Several coefficients measure an interaction effect between waiting time and additional factors related to the outside option: public transit availability, whether the trip is ordered on the street, and the presence of rain in the hour the trip was ordered. Because the last two trip-specific features interact with waiting time, their net effects are not immediately apparent. We compute marginal effects to see the impact: rainfall confers a 0.59% increase in the probability of choosing the outside option. On-street ordering is associated with a 0.16% increase. Consumers prefer to use the platform for longer-distance trips.

Table 3 shows price and waiting-time elasticities respectively and also a set of order-level elasticities, which measures only substitution to the outside option when either all prices or all wait-times change slightly. We see a general pattern that consumers are much more price elastic than waiting-time elastic: price elasticities range from four to eleven times higher, with starker differences in the evening.

In column 2, we use the estimated joint distribution of random coefficients to categorize four types of individuals as high (H) and low (L) sensitivity to price and waiting time. High-price-sensitivity individuals have *below*-median β_i^b, meaning they experience the highest utility from income. Likewise, high-waiting-time-sensitivity individuals have *below*-median β_i^w. Consumers have highly heterogeneous elasticities: between the two extreme groups, both price and waiting time elasticities differ by about a factor of four. We estimate a modest positive correlation between the sensitivity to price and waiting times: more price-sensitive consumers are also more waiting-time sensitive, and vice versa.

These elasticity estimates convey that both price and waiting time are important factors in

[23] Our estimates suggest that consumers value each rating point by \$0.10 and drivers' mean rating is 96.8/100, with standard deviation 1.43. We classify car types into three categories: basic, premium, and luxury. Premium cars (56% of our sample) include large cars, trucks and brands, such as Audi and Lexus. Luxury cars (10% of our sample) include brands such as Tesla and Ferrari. Luxury cars are estimated to have an average WTP of \$0.64 and premium cars have an average WTP of \$0.22 over basic cars.

Table 2: Model Coefficient Estimates

Description	Coefficient	Std Error
Price 6pm-6am	-1.183	0.002
Price 6am-6pm	-1.175	0.003
Waiting Time 1am-5am	-0.018	0.011
Waiting Time 6am-9am	-0.081	0.011
Waiting Time 10am-3pm	-0.089	0.01
Waiting Time 4pm-6pm	-0.062	0.01
Waiting Time 7pm-11pm	-0.031	0.01
Waiting × On-Street Order	-0.036	0.002
Waiting × Raining	0.015	0.004
Waiting Time Squared	-0.006	0.0002
Driver Rating Points	0.111	0.001
Car: Mid Quality	0.248	0.005
Car: High Quality	0.708	0.009
Trip Speed	-0.051	0.002
Alt. Transit Available	0.044	0.007
Order on Street	0.211	0.014
Rain	-0.148	0.034
Trip Distance	5.65	0.071
Waiting × Pickup Location FE 1-30		
Waiting × Dropoff Location FE 1-30		
Pickup Location FE 1-30	Omitted - See Figure B.3	
Dropoff Location FE 1-30		
Hour FE		

Note: Table 2 shows coefficient estimates and standard errors from the logit demand model for each consumer type. The final 120 rows are omitted for exposition. These parameter estimates comprise outside option shifters and waiting-time preference interactions with each of 30 pickup and dropoff locations as defined in Appendix A.2. The omitted results are instead depicted graphically in Figure B.3.

Table 3: Estimated Elasticities

Time of Day	Individual Type	Bid-Level Elasticities		Order-Level Elasticities	
		Price	Waiting Time	Price	Waiting Time
Daytime 6am-6pm	Overall	-4.37	-1.01	-3.9	-0.89
	H Price, H Wait Sensitivity	-8.59	-1.81	-7.36	-1.53
	H Price, L Wait Sensitivity	-2.86	-0.85	-2.8	-0.76
	L Price, H Wait Sensitivity	-5.1	-1.04	-4.47	-0.96
	L Price, L Wait Sensitivity	-2.03	-0.52	-2.06	-0.51
Evening 6pm-6am	Overall	-5.49	-0.5	-4.9	-0.49
	H Price, H Wait Sensitivity	-8.72	-0.8	-7.48	-0.75
	H Price, L Wait Sensitivity	-3.4	-0.37	-3.43	-0.37
	L Price, H Wait Sensitivity	-6.16	-0.52	-5.39	-0.52
	L Price, L Wait Sensitivity	-2.49	-0.22	-2.63	-0.24

Note: Table 3 shows the demand elasticity of price and waiting time across daytime and evening hours and individual type groupings. We distinguish as *high (H) price sensitivity* individuals who have below-median values for β_i^p and *low (L) price sensitivity* individuals as those with above-median values for β_i^p, and similarly for waiting-time sensitivity. The first two columns show these elasticities among competing bids, reflecting the change in demand due to a 1% change in price or waiting time on a single bid. The second two columns show the elasticities with respect to choosing the outside option, reflecting a change in demand due to a 1% change in price or waiting time on *all* bids.

the consumer's decisions, and that waiting-time elasticities vary throughout the day in ways that reflect the varying value of work and non-work tasks.[24]

5.2 Value-of-Time Results

We now present results on the value of time implied by our estimates, scaled to USD per hour. Recall that the VOT represents the difference between the value attainable at the trip *destination* and at the trip *origin*, given the activities and features of each location at each time for each person. We compute the VOT using the coefficients in Table 2 together with Equation 5, where we account for all trip-specific and environmental factors that affect valuations for the trip and the outside option, such as public transit and rainfall.

Table 4 summarizes the results. The overall mean VOT across all trips, expressed as an hourly quantity, is \$13.47. Underlying this average, there is significant individual-, time-of-day-, and location-specific heterogeneity. The most prominent of the three is the heterogeneity between individuals. As before, we report four groups of individuals, those with above- and below-median random coefficient estimates on both price and waiting-time preferences. The low-price-sensitivity and high-waiting-time-sensitivity group exhibits VOT nearly twice the overall average at \$23.39 per hour, whereas individuals with high sensitivity to price and low sensitivity to waiting time have an average VOT of \$5.00 per hour. All groups have similar time-of-day

[24] We can also decompose elasticities by trip origins and destinations as we have done in Table B.1. Broadly similar patterns between demand types are revealed, though each elasticity measure varies from one location to another. In general, price elasticities are more variable than waiting-time elasticities.

patterns, with the highest values in the morning between 6am and 9am. We find value-of-time estimates that are higher in the late morning and mid-day hours than in the evening and overnight. Finally, we divide Prague's spatial regions into *core* and *non-core*, where core regions are the locations including and adjacent to regions 11 and 20 as depicted in Figure A.2. In Table 4, we label as *urban core trips* any trip that involves one of these regions as either origin or destination. We find the VOT for trips in core regions is on average higher than for non-core trips. While there is meaningful variation in VOT both spatially and intertemporally, variation in the individual component of the value of time explains by far the largest share of its overall variation.

Our estimates of the value of time are larger than the average wage in Prague, which is approximately $9.50 per hour during the sample period.[25] This is perhaps not surprising, as taxi riders are typically positively selected on income and the users of the platform are likely to be more tech savvy. However, even for this selected set of riders, we find large dispersion in their VOT. As we illustrate in the next section, this dispersion has important implications for the pricing counterfactuals.

Table 4: Value-of-Time Estimates

Subsample	Value of Time (VOT)					
	12a–6a	6a–9a	10a–2p	3p–6p	7p–12a	All Hours
All Types	12.56	16.38	16.63	13.91	10.96	13.47
	(0.47)	(0.43)	(0.36)	(0.38)	(0.52)	(0.4)
H Price, H Wait Sensitivity	14.44	17.29	17.46	15.53	13.52	15.03
	(0.09)	(0.08)	(0.08)	(0.07)	(0.07)	(0.05)
H Price, L Wait Sensitivity	4.34	6.76	7.08	5.19	3.82	5.0
	(0.06)	(0.05)	(0.06)	(0.05)	(0.04)	(0.04)
L Price, H Wait Sensitivity	22.51	26.21	26.44	23.96	20.01	23.39
	(0.51)	(0.43)	(0.44)	(0.53)	(0.52)	(0.49)
L Price, L Wait Sensitivity	8.99	12.41	12.91	9.85	2.33	10.02
	(0.9)	(0.8)	(0.74)	(0.9)	(1.09)	(0.82)
Urban Core Trips	12.96	17.1	17.31	14.37	11.4	13.97
	(0.48)	(0.42)	(0.39)	(0.37)	(0.51)	(0.41)
Non Core Trips	9.93	11.78	9.61	10.57	7.6	9.94
	(0.62)	(0.53)	(0.36)	(0.39)	(0.56)	(0.5)

Note: Table 4 shows VOT estimates implied by the logit demand model. All estimates are presented in USD. We report bootstrap standard errors in parentheses, based on 100 bootstrap iterations.

Trip-specific heterogeneity Because in our discrete choice model preference parameters are individual, but not trip-specific, our VOT estimates for a given consumer are obtained by aver-

[25] Earnings data come from the Czech Statistical Office.

aging over all the trips the consumer takes. However, a given consumer may have a higher or lower VOT depending on the circumstances surrounding a ride (e.g., more or less urgent trips) and our VOT estimates average across all these circumstances. In Appendix B.6, we demonstrate that our data can be used to recover different VOT estimates between trips with a drop-off time close to the start of a new hour, which are more likely to involve deadlines, and those at different times. This analysis provides an example of how we might recover different types of trip-specific heterogeneity that is otherwise averaged in the results reported in Table 4.

Validation and comparison to other VOT measures: Our results provide insight into the interpretation of geographic (GPS) time-use data, such as cellphone location data. In several studies, authors use this type of data and interpret aggregate location decisions as a measure of location-specific amenities or productivity (see, e.g., Kreindler and Miyauchi, 2019; Athey et al., 2019). A natural question is, therefore, how close location values that are derived from GPS tracking are to our direct measures of the relative attractiveness of locations. To answer this question, we correlate our willingness to pay for waiting-time reductions when going from a to $\hat{a}$ with the fraction of all trips that go from a to $\hat{a}$. The two measures line up well. Figure B.6 in Appendix B.7 shows a scatter plot of the 900 different directional data points as well as the binscatter points on top. As the plot illustrates, the two measures are highly significantly correlated with a correlation coefficient of 0.56 and a *t-statistic* of 20.46.

5.3 Driver Pseudo-cost Results

Table 5 gives an overview of our driver pseudo-cost estimates. We find that drivers earn rents over their pseudo-costs as indicated by markups of around 30%. Winning drivers bid about \$1.37 lower on average than remaining drivers and have costs that are on average \$0.76 lower than the remaining drivers. We also find that drivers with lower wait times bid higher and, conditional on winning, earn higher markups than drivers with higher wait times. This suggests drivers are aware that low wait times are a quality attribute that makes their overall bid more competitive. The markup of drivers with the lowest wait time is more than 20% higher than those of other drivers. Within an order, the bid of the lowest-waiting-time driver has a higher markup than that of the driver with the highest rating. Interestingly, drivers with the highest rating bid 38 cents less, which is about 4% lower. These results suggest that the wait time premium is substantial and that high ratings are maintained in part by offering lower than average prices.

Large variance exists in the costs and markups that we recover. This finding suggests the platform's bidding mechanism plays an important role in discovering the lowest-cost drivers. A breakdown of cost by hour and by location in Figure 4 shows systematic variation in the average cost, with tight standard errors. However, these averages by location and hour mask

Table 5: Driver Cost Estimates

	Mean	Median	P25	P75	S.D.
Bid ($), winner	8.74	8.0	6.34	10.55	3.26
Bid ($), lowest wait	10.21	10.09	8.36	11.89	2.67
Bid ($), highest rating	9.53	9.43	7.8	11.08	2.49
Bid ($), all bidders	10.11	9.3	7.08	12.37	4.02
Cost ($), winner	6.28	6.09	4.86	7.47	1.94
Cost ($), all bidders	7.04	6.81	5.37	8.44	2.26
Markups winner	0.37	0.32	0.21	0.48	0.21
Markups all bidders	0.29	0.23	0.15	0.37	0.19
Markups lowest wait	0.33	0.28	0.18	0.44	0.21
Markups highest rating	0.32	0.27	0.17	0.43	0.21

Note: Table 5 provides a breakdown of markups and cost estimates that we recover from the inversion. The table also show summary statistics of prices for each of the breakdowns.

large variations across drivers. The gray shaded area represents one standard deviation above and below the average cost. Figure C.1 in Appendix C.2 shows that markups are highest during the day, especially in the early morning hours.

Figure 4: Pseudo-cost heterogeneity

(a) By Hour

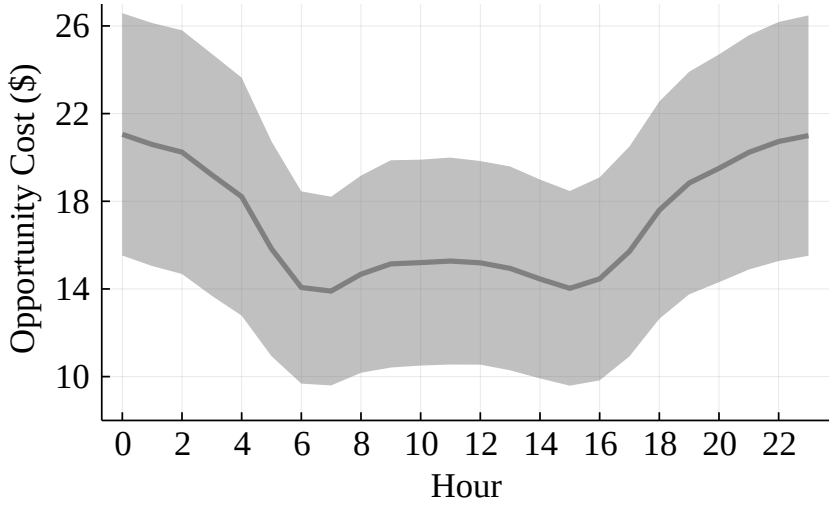

(b) By Location

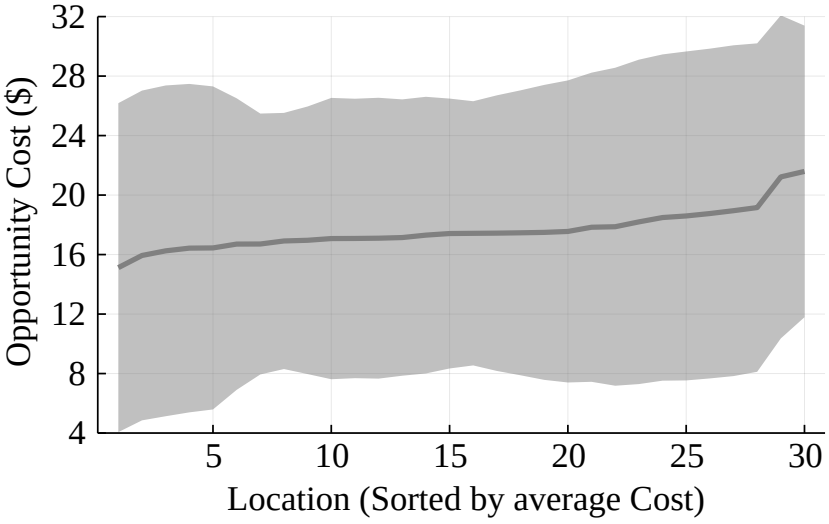

NOTE: Figure 4 shows the average of estimated driver costs by hour (panel 4a) and location (panel 4b). In Figure 4b, locations are ordered by average driver cost to better highlight the cost heterogeneity.

6 Pricing the Value of Time

Given our estimates of the underlying heterogeneity in both consumer VOT and driver opportunity costs, we analyze how much this heterogeneity matters for platform pricing. As ride-hail firms increasingly turn to non-linear pricing strategies and even offer ETA-based menu pricing,

we study the welfare implications of the platform's ability to exploit knowledge of its consumers' preferences over time and money.[26] In a series of counterfactuals, we let the platform procure drivers through different selection rules that resemble the baseline auction format. We then use our estimates to quantify the platform's profits and the overall welfare under a series of pricing policies that differ in how much information the platform uses about a consumer's behavior on the platform.

In what follows, we first describe how trip pricing and costs are determined, and the different pricing policies that we analyze in the counterfactuals:

Model of Platform Pricing In contrast to the current platform policy, where the platform collects a percentage fee and directly implements drivers' bids as prices, we now allow the platform to directly choose the price the rider faces. Figure 5 provides an illustration of this process.

Figure 5: Platform Pricing

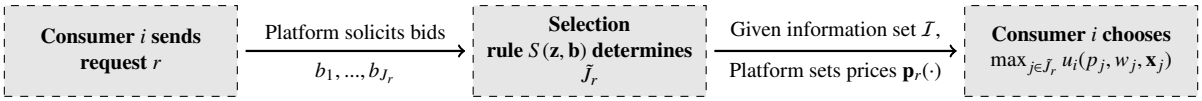

For each consumer request r, the platform receives bids from drivers in $\{1, \ldots, J_r\}$ with exogenous characteristics $\mathbf{z}_r = (\mathbf{z}_1, ..., \mathbf{z}_{J_r})$, which include the wait times, $\mathbf{w}_r = \{w_1, \ldots, w_{J_r}\}$, and other observable trip differences $\{\mathbf{x}_1, \ldots, \mathbf{x}_{J_r}\}$. As a function of the submitted bids and exogenous characteristics, the platform then selects drivers using a selection rule $S(\mathbf{z}_r, \mathbf{b}_r)$.[27] The selection rule determines the subset $\tilde{J}_r$ of drivers that the platform offers to the consumer.[28] The consumer then faces choice set $\{(p_j, \mathbf{z}_j) : j \in \tilde{J}_r\}$, where p_j is the price the consumer pays to the platform when choosing driver j. If the consumer chooses driver $j \in \tilde{J}_r$, the platform pays b_j to driver j and obtains profits equal to $p_j - b_j$.

To describe the platform's objective function given a set of bids, we need to specify the distribution over consumer preferences that the platform uses to calculate demand. In our counterfactual, we consider different pricing policies that vary in the information the platform uses about its consumers. We denote the platform's information set by $\mathcal{I}$, which determines the conditional distribution of preferences $\Phi(\cdot|\mathcal{I})$ used to calculate the probability that the consumer chooses a particular ride. Thus, under information set $\mathcal{I}$ and given a set of bids $\mathbf{b}_r$, the platform

[26] For example, Lyft recently introduced "wait and save," which grants a discount for riders who are willing to wait longer, in turn serving faster rides to consumers who have more urgent requests (https://www.ridester.com/lyft-wait-and-save/).

[27] Although the selection rule is *akin* to a scoring rule, we use the term selection for the following reason. Typically, in a scoring auction, participants are selected over *endogenously* chosen variables, such as prices and qualities. Instead, drivers only choose prices in our setting, whereas other relevant trip characteristics such as ETA, car make, and driver rating are fixed and observable to the platform at the time drivers submit their bids. Thus, our setting is closer to an asymmetric auction as in Mares and Swinkels (2014) than to a scoring auction.

[28] While drivers may choose bids conditional on the selection rule, the possibility of further bid manipulation (e.g., Bolotnyy and Vasserman, 2019) is nearly impossible, because drivers can only choose price and no other attributes of the bid.

sets prices to maximize profits:[29]

$$\mathbf{p}_r^*(\mathbf{b}_{\tilde{J}_r}, \mathbf{w}_{\tilde{J}_r}|\mathcal{I}) = \underset{(p_1,\ldots,p_{J_r})}{\arg\max} \sum_{j\in\tilde{J}_r} \mathbb{E}_{\tilde{\mathbf{x}}} \int \mathbb{P}\Big[j = \underset{j\in\tilde{J}_r}{\arg\max}\, u_i(p_j, w_{j,t}, \tilde{\mathbf{x}}_{j,t}; \boldsymbol{\beta})\Big]\, d\Phi(\boldsymbol{\beta}|\mathcal{I}) \cdot (p_j - b_j). \quad (18)$$

Driver adjustments Given the platform's selection rule S and pricing policy $\mathbf{p}_r$, drivers compete against each other by submitting bids. To compute drivers' optimal bidding behavior given the change in strategic incentives induced by the platform's pricing policy, we leverage the supply model and our estimates of drivers' opportunity costs introduced in Section 4. We provide details on the computations of counterfactual equilibria in Appendix D. Note that when drivers compute their bids, they may use information about demand-relevant variables, such as origin, destination, and time of day. Unlike the platform, however, they lack knowledge of the consumer's latent variables β_i^p and β_i^w, which are revealed by the consumer's order history and are accessible only to the platform.

Platform information sets and pricing policies The platform's information set $\mathcal{I}$ allows us to formalize the platform's ability to engage in different forms of price discrimination. In particular, we consider four information sets for the platform: (i) the null information set, $\overline{\mathcal{I}}$, in which the platform knows $\beta_i \sim \Phi$, but nothing else; (ii) the location-dependent information set, $\mathcal{I}_a$, in which the platform knows $\beta_i \sim \Phi(\cdot|a)$; (iii) the time-dependent information set, $\mathcal{I}_h$, in which the platform knows $\beta_i \sim \Phi(\cdot|h)$, when the consumer requests the ride at h; and (iv) the full information set, $\mathcal{I}^*$, where the platform knows the consumer's preferences β_i. We consider the following platform pricing policies:[30]

1. *Uniform pricing:* For each request, the platform offers a ride at a single price that depends only on the bid submitted by the selected driver. The platform selects the driver $j_u^\star$ that maximizes average consumer preferences. Given the selected driver's bid, $b_{j_u^\star}$ and using information set $\overline{\mathcal{I}}$, the platform implements a pricing function $p(b_{j_u^\star}|\overline{\mathcal{I}})$ that solves Equation 18.

2. *Third-degree price discrimination by location:* Similar to uniform pricing, the platform offers a ride at a single price that depends only on the selected driver's bid. Contrary to uniform pricing, the platform utilizes the distribution of consumer preferences conditional on each location to calculate its profits. Formally, the platform selects the driver $j_a^\star$ that maximizes average consumer preferences at location a. It then implements a pric-

[29] Whereas Equation 18 is written in terms of a final price that the consumer pays for the trip, in the counterfactual estimation these prices are implemented as a fixed tariff and a distance-based tariff. For notational simplicity and because it is not essential for the counterfactual comparisons, we simply present the resulting prices.

[30] Appendix D.1 provides further detail on the platform's policy.

ing function $p(b_{j_a^\star}|\mathcal{I}_a)$ for each location, which solves Equation 18 using the conditional distribution $\Phi(\cdot|a)$.

3. *Third-degree price discrimination by time of day:* For each time of day h, the platform selects the driver $j_h^\star$ that maximizes average consumer preferences during time of day h. The platform then implements a pricing function $p(b_{j_h^\star}|\mathcal{I}_h)$ for each hour of the day h, which solves Equation 18 using the conditional distribution $\Phi(\cdot|h)$.

4. *Menu pricing:* The platform offers the consumer a menu consisting of the lowest wait time and the lowest bid drivers, indexed j_f (*fast*) and j_c (*cheap*). The platform implements a pricing function $\mathbf{p}(b_{j_c}, b_{j_f}, \mathbf{w}_{\{j_c,j_f\}}|\overline{\mathcal{I}}) = (p_{j_c}(\cdot), p_{j_f}(\cdot))$, that determines the price at which the consumer can obtain the cheapest and the lowest wait time rides. The pricing function is chosen so as to maximize Equation 18, using the unconditional distribution of consumer preferences.

5. *Personalized Pricing:* The platform's information set is $\mathcal{I}^*$ so that the platform evaluates its profits knowing the consumer's preferences $\boldsymbol{\beta}$. Note, however, that the platform does not observe the logit shocks, so that the platform still faces uncertainty about whether a consumer would accept a given offer over the outside option. The platform picks the driver that maximizes average consumer preferences and implements a pricing function $p_i(b_{j_u^\star}|\mathcal{I}^*)$ that solves Equation 18 when $\mathcal{I} = \mathcal{I}^*$.

Before turning to the counterfactual results, two remarks are in order about the model of platform pricing:

First, drivers use their pseudo-costs to bid, which include their exogenous outside option and their continuation values at the baseline (recall Equation 15). Implicit in our formulation is that when choosing their bids, the drivers hold their continuation values fixed. This is justified by a small probability of requests on the platform and small differences in demand conditions across locations.[31] A more comprehensive analysis of the platform's pricing problem would also take into account how the change in the platform's policy affects drivers' continuation values, which in turn affects drivers' bidding incentives. Although this is outside the scope of the current paper, the decomposition result in Proposition 2 would allow us to conduct this computationally intensive exercise. In lieu of that, we present in Appendix D.4 a bounding exercise, which leverages the decomposition result in Proposition 2 to understand how changes in the partially endogenous part of the pseudo-cost (e) affects profits and welfare at the different counterfactuals. Note, however, that we recover the pseudo-costs from a fully dynamic model of driver behavior, which is key to obtaining credible estimates of the drivers' dynamic

[31] Recall that the endogenous portion of cost $e_{j,t}$ is the difference between staying put in the current location and the discounted value of starting at the destination of the trip that the driver bids for. If demand conditions across areas is small, then this difference should be small.

opportunity costs at a given location and time period that correctly reflect the platform's costs of procuring a ride.

Second, for computational reasons, we introduce three simplifications: (i) We do not allow the platform to search over all possible selection rules; (ii) we model the platform as a second mover, who chooses prices after the drivers submit their bids; and (iii) we abstract away from the dynamic implications of the platform's pricing problem. We choose these simplifications for tractability, because both the space of selection rules and computing equilibria for each scoring rule would not have been feasible. Furthermore, modeling the platform as a second mover allows us to provide a lower bound on the platform's profits from price discrimination. Indeed, this is the case that maximizes how much surplus the drivers can extract from the platform in response to the change in pricing policy. A more comprehensive analysis of platform centralization, which may include changes in the way drivers and consumers are matched, is not considered here.[32]

6.1 Counterfactual results

Table 6 summarizes the results from the counterfactual analysis. The first row describes the baseline results against which we compare the counterfactuals. For each counterfactual, we consider two versions of driver behavior. First are the results under the assumption that the platform faces the same distribution of bids as in the baseline. This *no driver adjustment* counterfactual allows us to assess the profit and welfare implications of the different platform pricing policies, holding the cost of supplying the rides fixed, similar to what one would do in a standard analysis of price discrimination. The second set of results demonstrate what happens once we allow drivers to optimally react to the change in the platform's policy. This *driver adjustment* counterfactual allows us to assess how much drivers' incentives undermine the platform's ability to benefit from price discrimination, by taking into account that the cost of supplying the rides is endogenous.

No driver adjustment Our first set of counterfactual results allows us to evaluate the nuanced effects of incorporating consumer information into pricing, while holding the costs of providing rides fixed. As stated above, these results tell us how different forms of price discrimination would affect welfare absent a driver reaction. Thus, the results can be interpreted as the direct effects of pricing on new information.

First, we document that the value to the platform of incorporating consumer information into its pricing is substantial. For instance, under personalized pricing, platform profits are about 3.4 times those at baseline and about 2.7 times those at uniform pricing. Instead, consumers and

[32] Such an analysis would require considering not just pricing but also the extent to which the platform may leverage control of the matching process. We study this problem separately in ongoing work.

drivers are worse off than under the baseline mechanism: the platform's ability to command higher prices and the subsequent downward distortions in quantities imply that consumer and driver surplus decrease by 37% and 56%, respectively, under personalized pricing relative to the baseline.

Second, our counterfactual results show that, conditional on the platform exercising its pricing power, drivers and consumers fare better under personalized pricing relative to uniform pricing. Because the platform can price discriminate consumers on the basis of their value of time, personalized pricing allows the platform to "price in" marginal VOT consumers, so that more rides are served than under uniform pricing. The platform mostly raises prices on high-VOT consumers and draws in additional low-VOT consumers. The average VOT of all consumers who choose the inside option choices is lowest under personalized pricing compared with all other pricing experiments, though it is still larger than at the baseline.

Third, in line with our demand model and our demand estimation results, we show that the platform does not benefit much from segmenting the market by location or time of day. Recall that the demand model's price coefficients vary only minimally within an individual consumer. Thus, across different location and/or time-of-day segments, the platform does not necessarily face different demand slopes, but rather intercepts. These intercepts capture, among other things, consumers' value of time. However, most of the variability of consumers' value of time is individual specific, rather than time of day or location specific. As we illustrate in Figure D.1 in Appendix D.3, the platform's pricing policy does vary with time-of-day or location, but the change is small.[33]

Finally, whereas personalized pricing is an extreme form of price discrimination on the basis of VOT, *menu pricing* is a simple policy that allows consumers to self-select on the basis of their VOT. Despite having additional price instruments than under uniform pricing, platform profits are lower under menu pricing when we do not allow drivers to adjust their bids. Contrary to our other counterfactuals, in which drivers get selected to maximize the consumer's average preferences, menu pricing selects the closest ride to the consumer and the cheapest ride to the platform. Under no driver adjustment, this reduces the available surplus to the consumers because of the wedge between the platform's price and the drivers' bids. This, in turn, limits the platform's ability to extract profits. The average VOT on the platform is the largest among all counterfactuals, highlighting that the high-VOT consumers are the ones whose choice sets are not severely distorted by the platform's selection rule.

Driver adjustment Our second set of counterfactual results relaxes the assumption of a fixed supply side, so that drivers now consider the platform's pricing policy when submitting bids.

[33]Recall that the uniform pricing and third-degree price discrimination counterfactuals use different driver selection rules. Thus, the platform cannot implement the uniform pricing policy under third-degree price discrimination. This is the reason that, counter to intuition, the platform's profits are lower under third-degree price discrimination than under uniform pricing.

The platform also accounts for drivers' endogenous bidding when determining its pricing policy. Thus, these results represent a combination of both direct and indirect effects of pricing on new information. This feature is missing from prior studies of price discrimination, which have so far focused on one-sided markets. We highlight how the interaction between the platform's pricing policy and drivers' bidding behavior both limits the profitability of price discrimination for the platform and also introduces new price and quantity distortions in the market.

The results suggest that although the platform still benefits from incorporating consumer information into its pricing, drivers' reactions imply lower platform profits by 15%–25%, except for menu pricing. Driver profits, however, increase relative to the no driver adjustment case. This result suggests that the platform must, in effect, compensate the drivers for the incentive costs implicit in each of the pricing policies.

Because of its different selection rule, menu pricing is the only pricing policy whereby this effect reverses. Once we allow drivers to adjust their bids, the platform's selection rule induces higher competition among drivers than at the baseline, because drivers have stronger incentives to underbid each other to be selected by the platform. Because most consumers pick the lowest-cost driver, drivers only serve the ride when they offer low prices, which induces them to bid more aggressively. Thus, menu pricing has a beneficial effect for the platform on both market sides, leading to higher profits than uniform pricing or third-degree price discrimination. However, driver profits slightly decrease with driver adjustment. While the average price increases once drivers adjust their bids, prices in the lower tail of the price distribution decrease as can be seen in Table 7. Lower prices in the left tail of the price distribution lead to a slight market expansion once drivers adjust their bids.

As in the case of no driver adjustment, the more information the platform incorporates into its pricing relative to uniform pricing, the greater the sum of consumer and driver surplus. Unlike the case of no driver adjustment, however, the drivers are the ones who really benefit from the more sophisticated pricing policies, claiming a larger proportion of the available surplus than under no driver adjustment. Instead, consumer welfare is largely negatively affected by the combination of the platform's price discrimination and the drivers' reactions: prices are higher than under no driver adjustment, leading to further downward quantity distortions. For instance, although personalized pricing allows the platform to price in marginal consumers, once we incorporate drivers' reactions, only 34% of the rides are actually served.

Table 6: Price Discrimination Counterfactual Results

Pricing Type	Avg. Platform Price	Surcharge	Driver Bid	Inside Option	Platform Profits per Order	Driver Profits per Order	Consumer Surplus	Average VOT Accepted Ride
Baseline (10% flat fee)	$9.83	-	$8.84	0.655	$0.55	$1.67	$1.29	$14.27
Uniform Pricing								
No Driver Adjustment	$11.13	-	$8.84	0.384	$1.12	$0.698	$0.79	$15.17
Driver Adjustment	$11.45	-	$9.93	0.336	$1.03	$0.747	$0.69	$15.16
Third-Degree by Location								
No Driver Adjustment	$11.17	-	$8.84	0.382	$1.11	$0.728	$0.78	$15.14
Driver Adjustment	$11.59	-	$9.86	0.339	$1.03	$0.759	$0.69	$15.14
Third-Degree by Hour								
No Driver Adjustment	$11.14	-	$8.84	0.383	$1.11	$0.702	$0.78	$15.15
Driver Adjustment	$11.48	-	$9.93	0.335	$0.96	$0.756	$0.69	$15.13
Menu Pricing								
No Driver Adjustment	$10.36	$0.84	$8.84	0.358	$1.0	$1.12	$0.71	$15.21
Driver Adjustment	$10.74	$1.04	$9.37	0.367	$1.11	$1.112	$0.75	$15.0
Personalized Pricing								
No Driver Adjustment	$11.18	-	$8.84	0.435	$2.31	$0.717	$0.82	$14.58
Driver Adjustment	$12.61	-	$10.0	0.34	$1.87	$0.778	$0.64	$14.73

Note: Table 6 summarizes the results of the pricing counterfactuals. Column 1, Average Platform Price, denotes the average price of all rides on the platform under each counterfactual. Column 2, Surcharge, shows the surcharge price charged over the regular tariff for the fastest trip in the menu. Column 3, Driver Bid, shows the average procurement cost submitted by each driver. Column 4 shows the percentage of rides offered by the platform that consumers accept. Columns 5-7 show the average welfare generated by each customer order, where the average is computed ex ante to the consumer selecting a trip or not. Finally, column 8 shows the average VOT associated with customers to accept the ride. Each counterfactual has two rows, *No Driver Adjustment*, in which driver bids are fixed as observed in the data, and *Driver Adjustment*, in which driver bids are re-optimized around the new platform pricing policy.

Table 7: Exploring the Price Distribution

	Q10	Q25	Q50	Q75	Q90
Baseline (10% flat fee)	$5.41	$6.83	9.01	$12.09	$15.32
Uniform Pricing					
No Driver Adjustment	$6.65	$8.01	$10.25	$13.57	$16.8
Driver Adjustment	$7.54	$8.64	$10.47	$13.36	$16.31
Third-Degree by Location					
No Driver Adjustment	$6.68	$8.03	$10.22	$13.5	$16.7
Driver Adjustment	$7.48	$8.6	$10.43	$13.32	$16.29
Third-Degree by Hour					
No Driver Adjustment	$6.65	$8.01	$10.25	$13.56	$16.78
Driver Adjustment	$7.55	$8.64	$10.47	$13.35	$16.3
Menu Pricing					
Cheapest, No Driver Adjustment	$6.57	$7.6	$9.52	$12.36	$15.1
Closest, No Driver Adjustment	$6.78	$8.01	$10.22	$13.51	$16.79
Cheapest, Driver Adjustment	$6.59	$7.59	$9.51	$12.14	$14.69
Closest, Driver Adjustment	$6.72	$7.8	$10.07	$13.22	$20.95
Third-Degree by Hour					
No Driver Adjustment	$6.55	$7.94	$10.09	$13.47	$17.08
Driver Adjustment	$7.68	$8.76	$10.51	$13.78	$21.83

Note: Table 7 summarizes the distribution of prices from the different pricing counterfactuals. Each row gives the corresponding quantiles of the respective counterfactuals. Each counterfactual has two rows, *No Driver Adjustment*, in which driver bids are fixed as observed in the data, and *Driver Adjustment*, in which driver bids are re-optimized around the new platform pricing policy.

Distributional effects The pricing policies have interesting distributional implications. Figure 6a shows consumer surplus in different counterfactual scenarios relative to the competitive baseline. A first observation is that although all consumers are hurt by the platform's new pricing strategies, the upper quartile of VOT, which has the highest surplus at the baseline, also fares best under all alternative pricing regimes. This quartile maintains more than 60% of baseline consumer surplus under all policies. Menu pricing and personalized pricing capitalize on high-VOT consumers and thereby equalize the surplus that different consumers earn in the market. However, Figure 6b shows that the platform captures higher surplus from higher VOT consumers under personalized pricing relative to uniform pricing. Consumers in the highest quartile of the VOT distribution lose almost 20% of consumer surplus under personalized pricing relative to

Figure 6: Distributional Effects of Policies

(a) Relative to Baseline

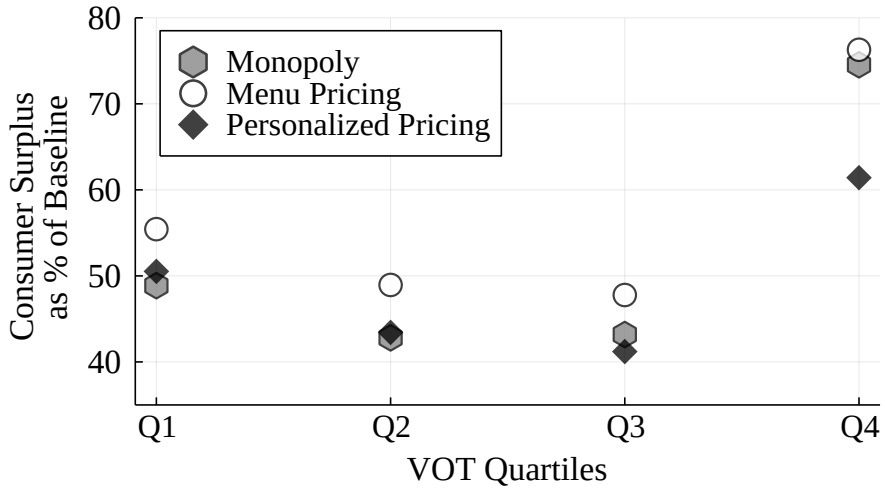

(b) Relative to Uniform Pricing

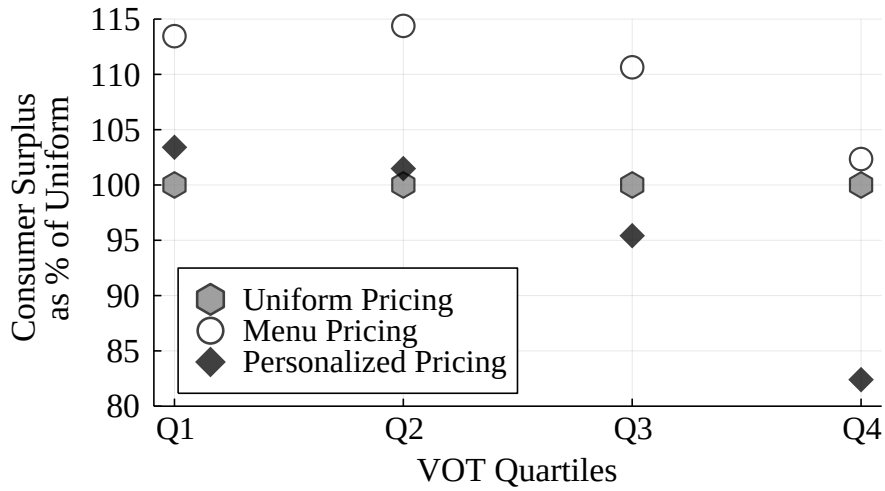

NOTE: Figure 6 shows for each quartile of the value-of-time distribution how consumer surplus changes relative to the baseline (panel 6a) and relative to uniform pricing (panel 6b) for uniform menu pricing, and personalized pricing.

uniform pricing. This can also be seen in Table 7, which shows that prices under both menu pricing and personalized pricing increase most in the upper end of the price distribution. This result highlights that more tailored pricing strategies lead to disproportionately higher prices for the consumer groups with the highest willingness to pay, whereas uniform pricing leads to nearly maximal rent extraction for the low willingness-to-pay segments.

7 Conclusions

The trade-off between time and money is at the heart of many important economic decisions. In this paper, we use data from a large European ride-share platform that offers menus with explicit trade-offs between time and money. We use this unique feature to estimate a demand model based on choices from these menus. This estimation allows us to recover riders' preferences and demand elasticities over time and money, as well as their implied willingness to pay to reduce waiting time.

Our demand model reveals noteworthy patterns in how individuals value time and money. Consumers are substantially more price elastic than waiting-time elastic. Large variation exists in the willingness to pay for waiting-time reductions in the population of riders. We show how these differences vary throughout the day; for instance, we show the willingness to pay for lower wait times is higher during work hours. Most of this variation is driven by latent demand characteristics across consumers as opposed to observable differences.

Our counterfactual analysis leverages the measured heterogeneity in the value of time to study the welfare implications of different forms of price discrimination on consumer welfare, driver welfare, and platform profits. We model the platform as procuring drivers through different driver-selection rules that resemble the baseline auction format. In contrast to the current platform policy, where the platform collects a percentage fee and directly implements drivers' bids as prices, we allow the platform to directly choose the price the rider faces.

Our counterfactual exercise accounts for a key feature of price discrimination in two-sided markets: because drivers have the opportunity to react to the platform's policy, the platform's costs of providing a ride is *endogenous* to its pricing policy. Thus, to evaluate drivers' reactions and the resulting welfare consequences, we pose and estimate a model of drivers' bidding behavior on the platform to infer drivers' opportunity cost of serving a ride. We demonstrate that dynamic bidding decisions can be transformed into a static auction, allowing us to recover driver opportunity costs through an estimator in the spirit of Guerre et al. (2000).

Our results underscore the nuanced welfare effects of incorporating detailed consumer information into pricing and the new frictions that arise because of the two-sided nature of our market. Our uniform pricing results show that the platform has unexercised pricing power, which comes at a considerable welfare cost for consumers and drivers. Furthermore, conditional on using its pricing power, total surplus is higher the more information the platform incorporates into its pricing. Although the value of information to the platform is substantial, consumers and drivers also benefit from the increased use of information relative to uniform pricing: more information allows the platform to price in low-VOT individuals, increasing the number of rides served by the platform. Finally, once we take into account drivers' optimal reaction to the platform's policy, drivers are the big beneficiaries of the platform's increased use

of information, to the detriment of platform profits and even more so to consumer surplus. Our results highlight that conclusions about welfare and profit implications of price discrimination in two-sided markets depend on its effects on both market sides.

References

Abrantes, P. A. and M. R. Wardman (2011): "Meta-analysis of UK values of travel time: An update," *Transportation Research Part A: Policy and Practice*, 45, 1–17.

Aguiar, M. and E. Hurst (2007): "Life-cycle prices and production," *American Economic Review*, 97, 1533–1559.

Aguiar, M., E. Hurst, and L. Karabarbounis (2012): "Recent developments in the economics of time use," *Annu. Rev. Econ.*, 4, 373–397.

Aguirre, I., S. Cowan, and J. Vickers (2010): "Monopoly price discrimination and demand curvature," *American Economic Review*, 100, 1601–15.

Ali, S. N., G. Lewis, and S. Vasserman (2020): "Voluntary disclosure and personalized pricing," in *Proceedings of the 21st ACM Conference on Economics and Computation*, 537–538.

Aridor, G., Y.-K. Che, and T. Salz (2021): "The Effect of Privacy Regulation on the Data Industry: Empirical Evidence from GDPR," in *Proceedings of the 22nd ACM Conference on Economics and Computation*, 93–94.

Arnott, R., A. De Palma, and R. Lindsey (1993): "A structural model of peak-period congestion: A traffic bottleneck with elastic demand," *American Economic Review*, 161–179.

Athey, S., B. Ferguson, M. Gentzkow, and T. Schmidt (2019): "Experienced Seggregation," Tech. rep.

Bauner, C. (2015): "Mechanism choice and the buy-it-now auction: A structural model of competing buyers and sellers," *International Journal of Industrial Organization*, 38, 19–31.

Becker, G. S. (1965): "A Theory of the Allocation of Time," *The Economic Journal*, 493–517.

Belenky, P. (2011): "Revised departmental guidance on valuation of travel time in economic analysis," *US Department of Transportation. Washington, DC*.

Bento, A., K. Roth, and A. R. Waxman (2020): "Avoiding traffic congestion externalities? The value of urgency," *National Bureau of Economic Research*.

Bergemann, D., B. Brooks, and S. Morris (2015): "The limits of price discrimination," *American Economic Review*, 105, 921–57.

Bloom, N., J. Liang, J. Roberts, and Z. J. Ying (2015): "Does working from home work? Evidence from a Chinese experiment," *Quarterly Journal of Economics*, 130, 165–218.

Bolotnyy, V. and S. Vasserman (2019): "Scaling auctions as insurance: A case study in infrastructure procurement," *NBER Working Paper, January*, 8.

Borjesson, M., M. Fosgerau, and S. Algers (2012): "On the income elasticity of the value of travel time," *Transportation Research Part A: Policy and Practice*, 46, 368 – 377.

Brancaccio, G., M. Kalouptsidi, and T. Papageorgiou (2017): "Geography, Search Frictions and Endogenous Trade Costs," .

Brancaccio, G., M. Kalouptsidi, T. Papageorgiou, and N. Rosaia (2020): "Search Frictions and Efficiency in Decentralized Transport Markets," Tech. rep., mimeo, Harvard University.

Buchholz, N. (2018): "Spatial Equilibrium, Search Frictions and Dynamic Efficiency in the Taxi Industry," .

Camerer, C., L. Babcock, G. Loewenstein, and R. Thaler (1997): "Labor supply of New York City cabdrivers: One day at a time," *Quarterly Journal of Economics*, 407–441.

Castillo, J. C. (2019): "Who Benefits from Surge Pricing?" *Available at SSRN 3245533*.

Chen, M. K., J. A. Chevalier, P. E. Rossi, and E. Oehlsen (2017): "The value of flexible work: Evidence from uber drivers," Tech. rep., National Bureau of Economic Research.

Cirillo, C. and K. W. Axhausen (2006): "Evidence on the distribution of values of travel time savings from a six-week diary," *Transportation Research Part A: policy and practice*, 40, 444–457.

Cohen, P., R. Hahn, J. Hall, S. Levitt, and R. Metcalfe (2016): "Using big data to estimate consumer surplus: The case of uber," *National Bureau of Economic Research*.

Couture, V., G. Duranton, and M. A. Turner (2018): "Speed," *Review of Economics and Statistics*, 100, 725–739.

Crawford, V. P. and J. Meng (2011): "New york city cab drivers' labor supply revisited: Reference-dependent preferences with rationalexpectations targets for hours and income," *American Economic Review*, 101, 1912–1932.

Domencich, T. A. and D. McFadden (1975): "Urban travel demand-a behavioral analysis," Tech. rep.

Doval, L. and V. Skreta (2021): "Purchase history and product personalization," .

Dubé, J.-P. and S. Misra (2019): "Personalized pricing and customer welfare," *Available at SSRN 2992257*.

Farber, H. S. (2005): "Is Tomorrow Another Day? The Labor Supply of New York City Cabdrivers," *Journal of Political Economy*, 113, 46–82.

——— (2008): "Reference-dependent preferences and labor supply: The case of New York City taxi drivers," *American Economic Review*, 98, 1069–1082.

Fosgerau, M., K. Hjorth, and S. V. Lyk-Jensen (2007): "The Danish Value of Time Study," Tech. rep., Danmarks Transportforskning, Report 5.

Frechette, G. R., A. Lizzeri, and T. Salz (2018): "Frictions in a competitive, regulated market: Evidence from taxis," Tech. rep., National Bureau of Economic Research.

Freund, D. and G. van Ryzin (2021): "Pricing Fast and Slow: Limitations of Dynamic Pricing Mechanisms in Ride-Hailing," Tech. rep., SSRN.

Gaineddenova, R. (2021): "Pricing and Efficiency in a Decentralized Ride-Hailing Platform," Tech. rep., University of Wisconsin, Madison.

Goldszmidt, A., J. A. List, R. D. Metcalfe, I. Muir, V. K. Smith, and J. Wang (2020): "The Value of Time in the United States: Estimates from Nationwide Natural Field Experiments," Tech. rep., National Bureau of Economic Research.

Guerre, E., I. Perrigne, and Q. Vuong (2000): "Optimal nonparametric estimation of first-price auctions," *Econometrica*, 68, 525–574.

Hall, J. D. (2018): "Pareto improvements from Lexus Lanes: The effects of pricing a portion of the lanes on congested highways," *Journal of Public Economics*, 158, 113–125.

Hall, J. V., J. J. Horton, and D. T. Knoepfle (2019): "Pricing Efficiently in Designed Markets: The Case of Ride-Sharing," .

Hendel, I. and A. Nevo (2013): "Intertemporal price discrimination in storable goods markets," *American Economic Review*, 103, 2722–51.

Hortacsu, A. and D. McAdams (2010): "Mechanism choice and strategic bidding in divisible good auctions: An empirical analysis of the turkish treasury auction market," *Journal of Political Economy*, 118, 833–865.

Jara-Diaz, S. R., M. A. Munizaga, P. Greeven, R. Guerra, and K. Axhausen (2008): "Estimating the value of leisure from a time allocation model," *Transportation Research Part B: Methodological*, 42, 946 – 957.

Jofre-Bonet, M. and M. Pesendorfer (2003): "Estimation of a dynamic auction game," *Econometrica*, 71, 1443–1489.

Kehoe, P. J., B. J. Larsen, and E. Pastorino (2018): "Dynamic competition in the era of big data," Tech. rep., Stanford University Stanford.

Kreindler, G. and Y. Miyauchi (2019): "Measuring commuting and economic activity inside cities with cell phone records," Tech. rep., Working paper.

Kreindler, G. E. (2018): "The welfare effect of road congestion pricing: Experimental evidence and equilibrium implications," *Unpublished paper*.

Levitt, S. D., J. A. List, S. Neckermann, and D. Nelson (2016): "Quantity discounts on a virtual good: The results of a massive pricing experiment at King Digital Entertainment," *Proceedings of the National Academy of Sciences*, 113, 7323–7328.

List, J. A. (2004): "The nature and extent of discrimination in the marketplace: Evidence from the field," *Quarterly Journal of Economics*, 119, 49–89.

Liu, T., Z. Wan, and C. Yang (2019): "The efficiency of a dynamic decentralized two-sided matching market," *Available at SSRN 3339394*.

Luo, Y., I. Perrigne, and Q. Vuong (2018): "Structural analysis of nonlinear pricing," *Journal of Political Economy*, 126, 2523–2568.

Mares, V. and J. M. Swinkels (2014): "On the analysis of asymmetric first price auctions," *Journal of Economic Theory*, 152, 1–40.

Mas, A. and A. Pallais (2017): "Valuing alternative work arrangements," *American Economic Review*, 107, 3722–59.

McFadden, D. (1974): "The measurement of urban travel demand," *Journal of public economics*, 3, 303–328.

Miller, T. R. (1989): *The Value of Time and the Benefit of Time Saving: A Literature Synthesis and Recommendations on Values*, Urban Institute.

Miravete, E. J. (1996): "Screening consumers through alternative pricing mechanisms," *Journal of Regulatory Economics*, 9, 111–132.

NEVO, A., J. L. TURNER, AND J. W. WILLIAMS (2016): "Usage-based pricing and demand for residential broadband," *Econometrica*, 84, 411–443.

NEVO, A. AND A. WONG (2019): "The elasticity of substitution between time and market goods: Evidence from the Great Recession," *International Economic Review*, 60, 25–51.

PETRIN, A. AND K. TRAIN (2010): "A control function approach to endogeneity in consumer choice models," *Journal of marketing research*, 47, 3–13.

PIGOU, A. C. (1920): *The Economics of Welfare*, Macmillan.

ROSAIA, N. (2020): "Competing platforms and transport equilibrium: Evidence from New York City," Tech. rep., mimeo, Harvard University.

ROSSI, P. E. AND G. M. ALLENBY (2003): "Bayesian Statistics and Marketing," *Marketing Science*, 22, pp. 304–329.

ROSSI, P. E., G. M. ALLENBY, AND R. MCCULLOCH (2005): *Bayesian Statistics and Marketing*, Wiley.

ROSSI, P. E., R. E. MCCULLOCH, AND G. M. ALLENBY (1996): "The value of purchase history data in target marketing," *Marketing Science*, 15, 321–340.

SHILLER, B. R. (2013): "First degree price discrimination using big data," Tech. rep.

SMALL, K. A. (1982): "The scheduling of consumer activities: work trips," *American Economic Review*, 72, 467–479.

——— (2012): "Valuation of travel time," *Economics of Transportation*, 1, 2 – 14.

TANNER, M. A. AND W. H. WONG (1987): "The Calculation of Posterior Distributions by Data Augmentation," *Journal of the American Statistical Association*, 82, 528–540.

THAKRAL, N. AND L. T. TØ (2017): "Daily Labor Supply and Adaptive Reference Points," .

TRAIN, K. E. (2009): *Discrete Choice Methods with Simulation*, Cambridge University Press.

TSENG, Y.-Y. AND E. T. VERHOEF (2008): "Value of time by time of day: A stated-preference study," *Transportation Research Part B: Methodological*, 42, 607–618.

WALDFOGEL, J. (1995): "The selection hypothesis and the relationship between trial and plaintiff victory," *Journal of Political Economy*, 103, 229–260.

Online Appendix

A Platform and Data Details

A.1 Interface

Figure A.1 shows Liftago's app interface:

Figure A.1: Liftago app's interface

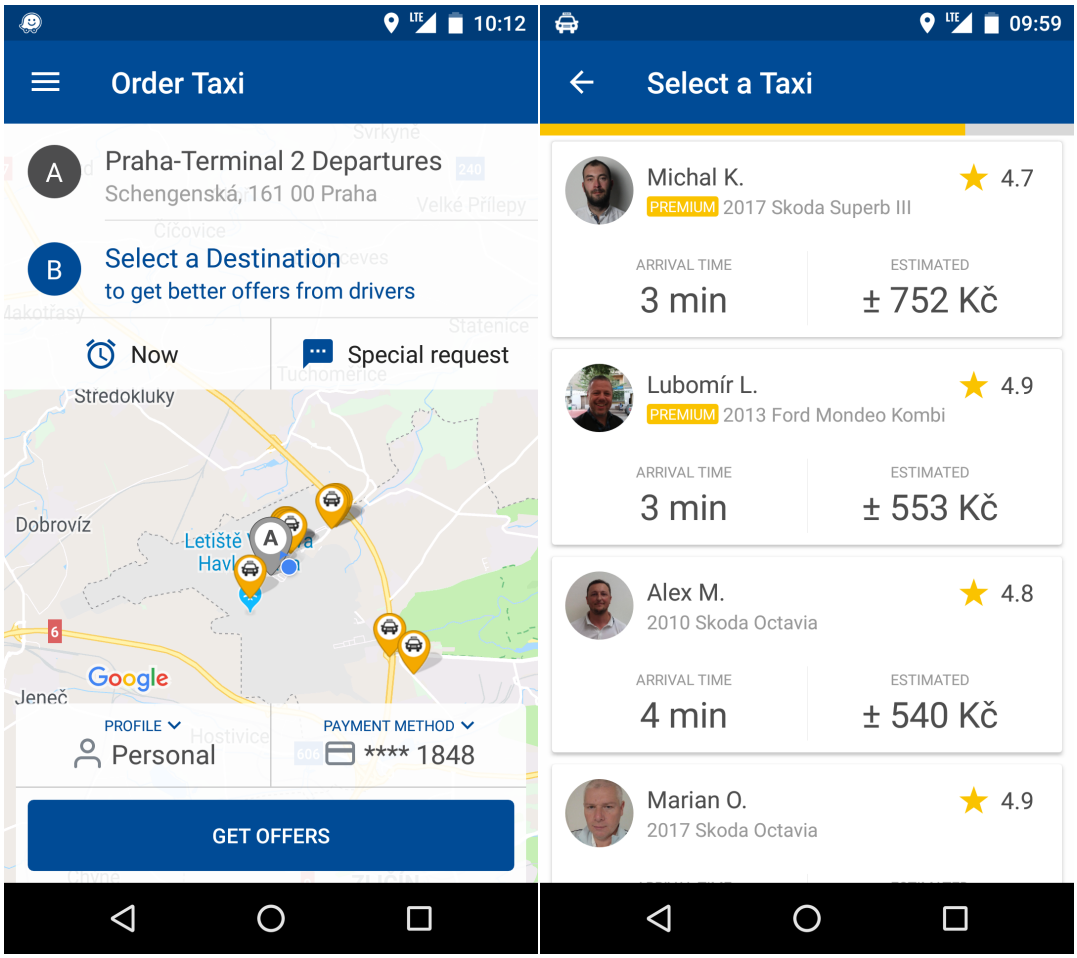

A.2 Locations

Using the exact GPS points of trip origin, we partition our data into 30 locations. Figure A.2 shows these locations together with an index value for comparing the results in Section 5. The partitioning is done according to a simple *k-means* clustering procedure on the requested pickup locations with $k = 30$. This procedure minimizes the straight-line distance between each point and the weighed center of all points within the same cluster, with the constraint that

each cluster has an equal number of points. The depicted locations are close approximations of the k-means clustering procedure, displayed as Voronoi cells that contain the clustered points. This process allows location definitions to be independent of any political boundaries and better representative of places in which demand is concentrated.

Figure A.2: Locations in Prague

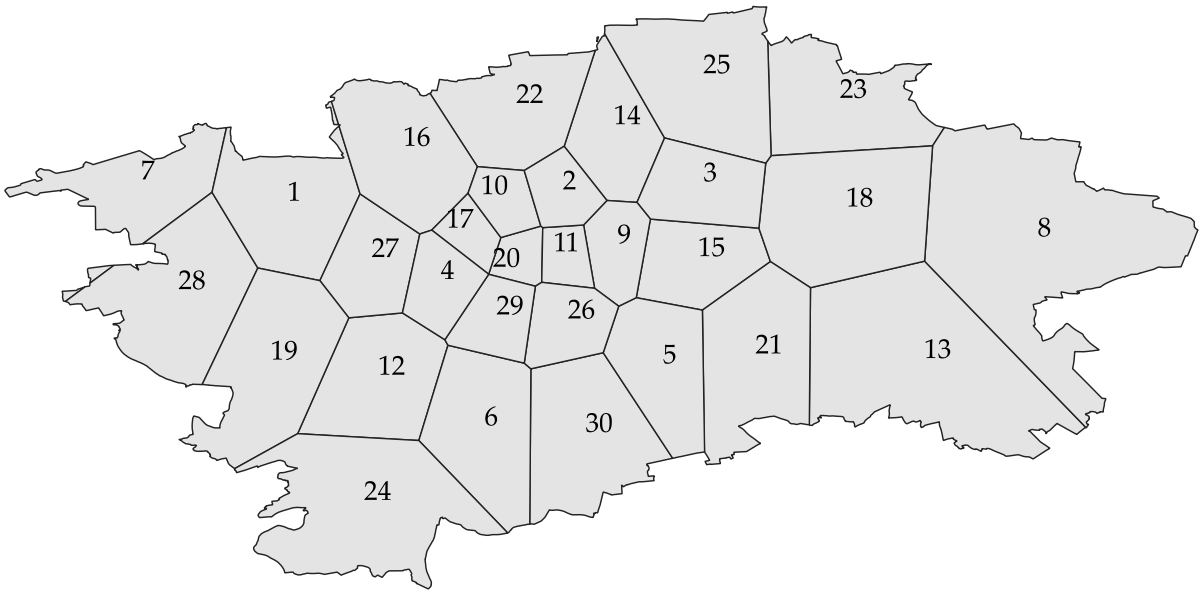

Note: Figure A.2 maps the boundaries of the city of Prague with locations defined by a kmeans-clustering procedure on GPS-locations of trip origins and depicted as Voronoi cells that contain the clustered points. Displayed index values correspond to indices used in the paper.

A.3 Market Time Series Summary

Figure A.3 summarizes the week-over-week trends in prices. Beginning 2017, the number of consumers and drivers on the platform stops growing and enters a relatively stationary period, although there still are large swings in the number of consumers towards the end of 2017. Figure A.3 shows the relationship between labor supply and price during the sample period. Figure A.3a shows how average waiting time and average price evolve during the sample period and Figure A.3b shows how the driver count and average price evolve during the sample period. As expected, price decreases as supply increases during the winter holiday seasons and increases as supply falls during the summer.

Figure A.3: Weekly Waiting Times and Number of Drivers Compared to Prices

(a) Wait time vs. Prices

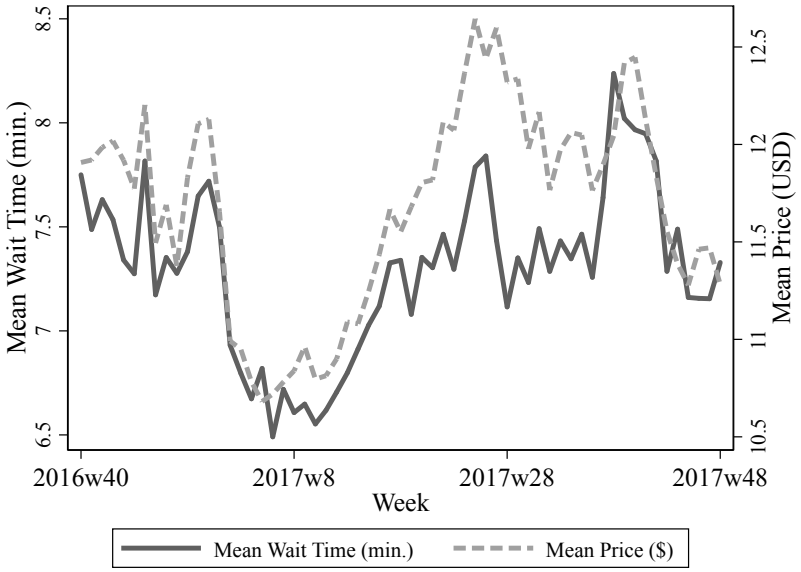

(b) Driver count vs. Prices

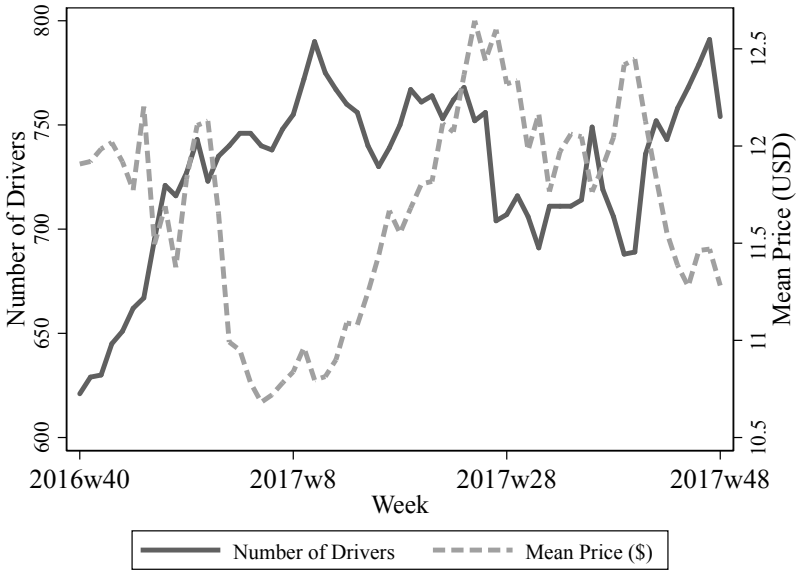

NOTE: Figure A.3 displays the average offered waiting time and the total number of unique drivers in each week beginning October 2016 to December 2017. Both series are compared against the average offered prices.

B Demand side: omitted figures and results

B.1 Choices and Trade-offs

Figure B.1 shows the proportion of trips that involve a trade-off between spending less and waiting less by hour:

Figure B.1: Trips with Price - Wait Time Trade-off by Hour

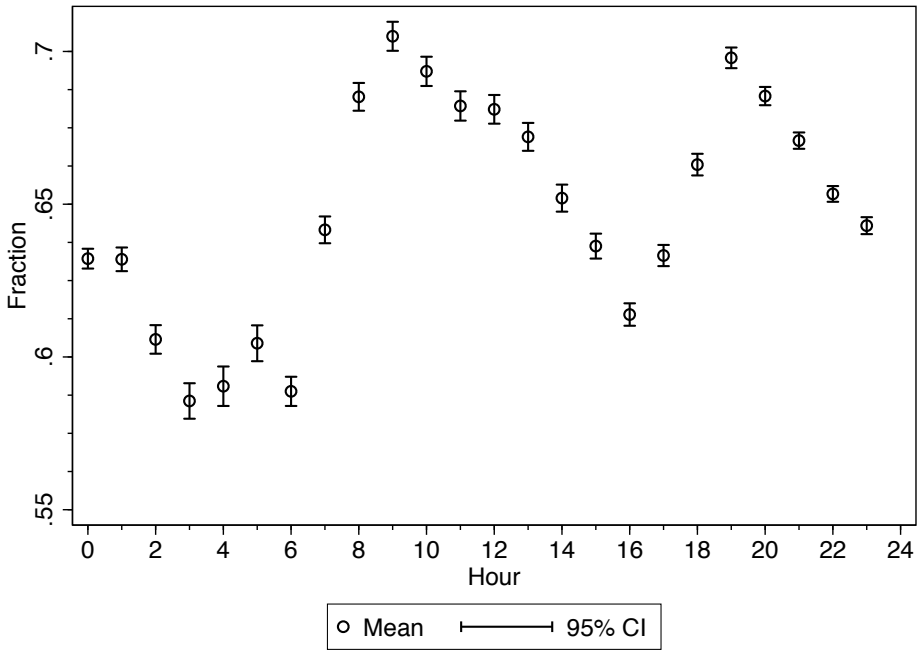

Linearity of choice probability in waiting time Figure B.2 provides further detail about the probability of choosing to take a trip on the platform. Figure B.2a shows the probability of choosing a trip as a function of the wait time, residualized after taking into account time of day, origin and destination location, weather conditions, and the respective other prices and wait times. Instead, Figure B.2b shows the probability of choosing any trip over the outside option as a function of the minimum waiting time, residualized for time of day, origin and destination locations, and weather conditions.

Figure B.2: Choices as a Function of Wait Time

(a) Trip Choice as Function of Waiting Time

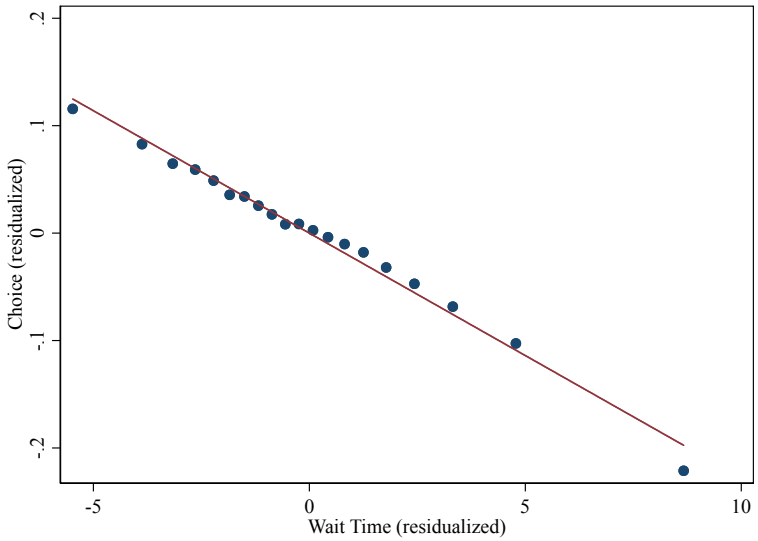

(b) Trip Choice as Function of Minimum Waiting Time

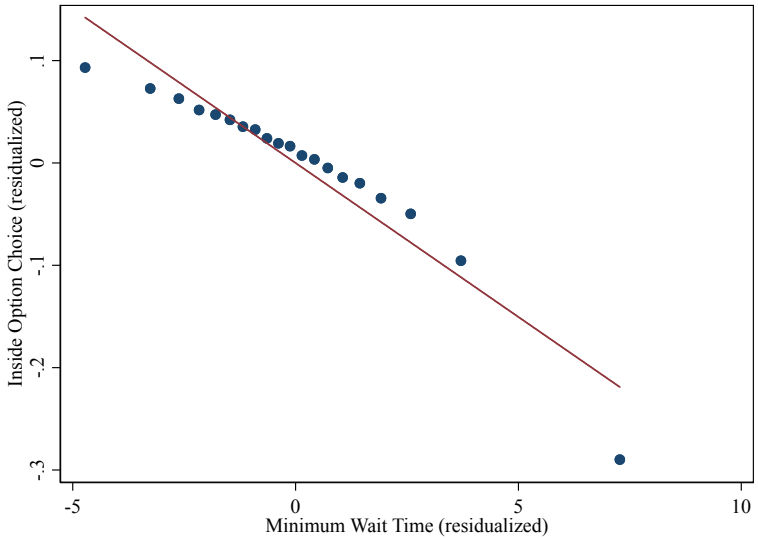

B.2 Location Parameter Estimates

Here we offer additional details on location-specific parameter estimates. Figure B.3 summarizes all location-specific waiting-time and price coefficient estimates omitted from Table 2. Because each location contains multiple consumers and each consumer has individual preference estimates, we report each location-specific estimate as a bar. The dark line shows the median estimate and the vertical bars around each point display the 10th and 90th percentiles of all individual estimates within the location as indicated on the horizontal axis. Location indices

may be cross-referenced with Figure A.2. Figure B.3a displays the waiting time coefficients and Figure B.3b displays the price coefficients.

Figure B.3: Location-Specific and Time Specific Coefficient Estimates

(a) Waiting Time Coefficients

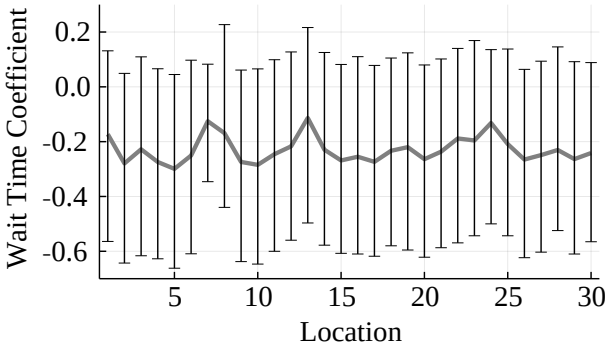

(b) Price Coefficients

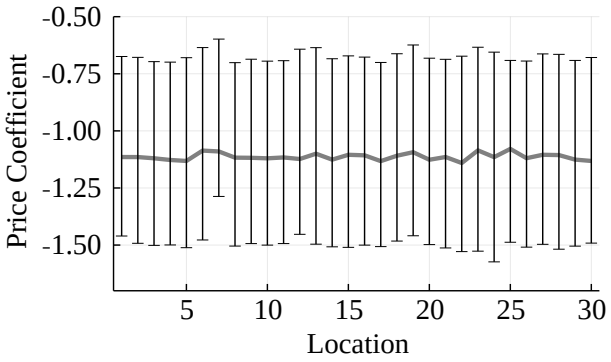

Note: This figure summarizes all location-specific waiting-time and price coefficient estimates.

B.3 Time of Day Parameter Estimates

Here we offer additional details on time-of-day-specific parameter estimates. Figure B.4 summarizes all time-of-day-specific waiting-time and price coefficient estimates omitted from Table 2. Similarly to the analysis in Appendix B.2, we report each time-of-day-specific estimate as a bar. The dark line shows the median estimate and the vertical bars around each point display the 10th and 90th percentiles of all individual estimates within the hour indicated. Figure B.3a displays the waiting time coefficients and Figure B.3b displays the price coefficients.

Figure B.4: Location-Specific and Time Specific Coefficient Estimates

(a) Waiting Time Coefficients

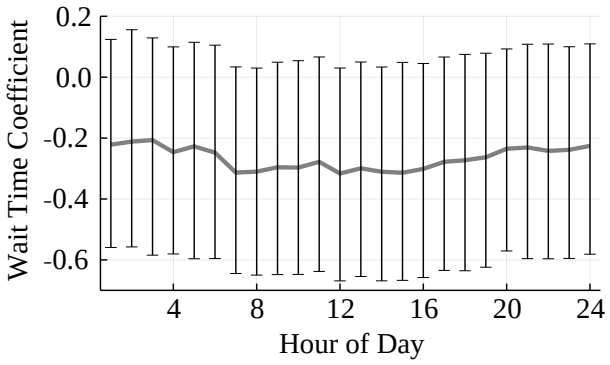

(b) Price Coefficients

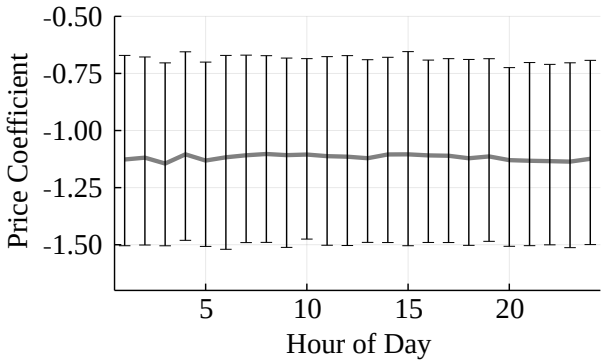

Note: This figure summarizes all hour-specific waiting-time and price coefficient estimates.

B.4 Elasticities by Area

Table B.1 below presents the price and waiting time elasticity estimates by origin and destination areas. For example, area 1's origin elasticities are the price and waiting time elasticity associated with all trips that depart from area 1. Similarly, area 1's destination elasticities obtain from all trips that arrive to area 1. Recall that location indices may be found in Figure A.2.

Table B.1: Bid Level Elasticities by Origin and Destination Area

	Origin Areas		**Destination Areas**	
Location Index	Price	Waiting Time	Price	Waiting Time
1	-6.47	-0.87	-5.71	-0.63
2	-3.94	-0.64	-3.41	-0.82
3	-5.47	-0.89	-5.05	-0.64
4	-4.44	-0.66	-3.79	-0.81
5	-5.99	-0.93	-5.48	-0.62
6	-6.6	-1.04	-6.39	-0.54
7	-11.69	-0.44	-11.34	-0.96
8	-12.67	-1.25	-10.0	-0.49
9	-3.77	-0.75	-3.78	-0.69
10	-4.0	-0.61	-3.57	-0.78
11	-3.44	-0.49	-3.22	-0.72
12	-7.13	-1.15	-5.99	-0.49
13	-9.66	-1.04	-8.49	-0.48
14	-5.4	-0.81	-5.0	-0.64
15	-4.87	-0.92	-4.58	-0.65
16	-5.09	-0.8	-4.3	-0.72
17	-4.38	-0.62	-3.74	-0.87
18	-8.11	-1.39	-7.28	-0.64
19	-7.19	-0.97	-6.4	-0.61
20	-3.77	-0.51	-3.56	-0.88
21	-6.99	-1.02	-6.6	-0.57
22	-6.69	-0.98	-5.59	-0.54
23	-9.27	-1.35	-7.3	-0.41
24	-11.76	-1.21	-9.45	-0.55
25	-8.04	-1.05	-7.05	-0.61
26	-4.15	-0.68	-4.0	-0.73
27	-5.16	-0.91	-4.39	-0.67
28	-8.28	-0.93	-7.37	-0.51
29	-4.16	-0.6	-3.81	-0.69
30	-6.69	-0.94	-5.96	-0.57

Note: Table B.1 shows price and waiting time elasticities across the thirty different areas of Prague for areas as origins and destinations.

B.5 Control Function: details

We now provide further detail on the control function approach used to estimate our demand model:

B.5.1 Driver fixed effects for Control Function Approach

Figure B.5 depicts the distribution of estimated driver fixed effects used to construct the control function:

Figure B.5: Driver Fixed Effects

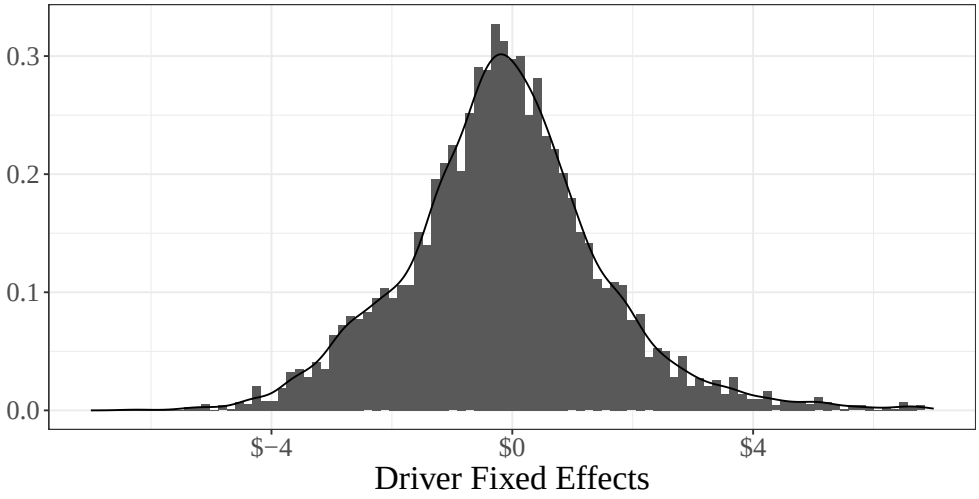

B.5.2 Estimation Results Omitting Control Function

Table B.2 below presents the price and waiting time elasticity estimates in which the control function is omitted. This table replicates Table 3 except that the model is estimated with no control function. We distinguish as *high (H) price sensitivity* individuals who have below median values for β_i^p and *low (L) price sensitivity* individuals as those with above median values for β_i^p, and similarly for waiting time sensitivity. The first two columns show these elasticities among competing bids, reflecting the change in demand due to a 1% change in price or waiting time on a single bid. The second two columns show them with respect to choosing the outside option, reflecting a change in demand due to a 1% change in price or waiting time on *all* bids.

Table B.2: Estimated Elasticities

Time of Day	Individual Type	Bid Level Elasticities		Order Level Elasticities	
		Price	Waiting Time	Price	Waiting Time
Daytime 6am-6pm	Overall	-1.83	-0.63	-1.74	-0.64
	H Price, H Wait Sensitivity	-4.08	-1.18	-3.83	-1.09
	H Price, L Wait Sensitivity	-0.95	-0.51	-1.04	-0.53
	L Price, H Wait Sensitivity	-2.15	-0.6	-2.05	-0.68
	L Price, L Wait Sensitivity	-0.65	-0.3	-0.75	-0.38
Evening 6pm-6am	Overall	-2.58	-0.25	-2.4	-0.28
	H Price, H Wait Sensitivity	-4.32	-0.39	-4.12	-0.4
	H Price, L Wait Sensitivity	-1.25	-0.2	-1.33	-0.22
	L Price, H Wait Sensitivity	-3.09	-0.26	-2.87	-0.31
	L Price, L Wait Sensitivity	-1.04	-0.15	-1.12	-0.18

Note: Table B.2 shows the demand elasticity of price and waiting time across daytime and evening hours and individual type groupings.

B.6 Trip-Specific Heterogeneity Results

The baseline results in Table 4 show the average VOT across different hours of the day. Within each time-of-day and within each individual's *type*, however, there is additional heterogeneity due to the fact that some trips are more or less time-sensitive. For example, a given person may express higher VOT if she is late for an appointment.

To analyze this type of heterogeneity, we define *time-sensitive* trips as the subset of trips in which having requested a ride, a consumer faces a set of bids in which (1) the arrival time falls around a rounded hour increment such as 9:00am or 2:00pm, (2) only one bid would provide a trip that arrives before the hour, while all others would provide a trip which arrives after the hour, and (3) a trip occurs on the platform. Because the VOT estimated on trips generated on this subset is inherently selected due to point (3), we compare this against a similar subset of trips around a placebo clock-time. We thus define *placebo* trips by selecting orders where the arrival time falls around a clock time ending in :23 or :53, such as 8:23am or 2:53pm. We then apply criteria (2) and (3) to these trips. The difference in VOT between time-sensitive and placebo trips reveals the relevant heterogeneity in time-sensitivity.

To augment our baseline results, Table B.3 reports results for *time sensitive* trips and shows that the VOT for this subset is about 58% greater than the comparable measure in the placebo group. The first column reports VOT for all trips, as in Table 4, as a comparison. Our baseline VOT results, therefore, can be interpreted as averages across this type of trip-specific heterogeneity.

Table B.3: Trip-Specific Heterogeneity in VOT

	All Trips	Time-Selected Trips	
		Placebo	*Time-Sensitive*
VOT ($/hour)	$13.47	$17.92	$28.34
N Trips	1,021,007	86,786	62,229
N Individuals	80,161	32,438	21,651

NOTE: Table B.3 shows baseline mean VOT estimates in the first column. The second column reports mean VOT estimates for trips in which exactly one bid occurs before the 23rd and 53rd minute of each hour and additional bids fall beyond this time. The third column similarly reports VOT estimates for trips in which exactly one bid occurs before the first minute of each hour. All estimates are presented in US dollars.

B.7 Correlation between VOT and Travel Flows

Our analysis is, to our knowledge, the first to pair highly granular spatial data, which records where people go within a city, with direct VOT measures, which capture the relative attractiveness of locations as per our illustration in Figure 3. A natural question is, therefore, how close location values that are derived from GPS tracking are to our direct measures of the relative attractiveness of locations. To answer this question we correlate our WTP for waiting time reductions when going from a to $\hat{a}$ with the fraction of all trips that go from a to $\hat{a}$. The two measures line up well. Figure B.6 shows a scatter plot of the nine hundred different directional data points as well as the binscatter points on top. As the plot illustrates, the two measures are highly significantly correlated with a correlation coefficient of 0.56 and a *t-statistic* of 20.46. This correlation is highest during the middle of the day and lowest at midnight.

These results convey that travel flows appear to be a good but not perfect measure of time valuations. The variation in the correlation between our VOT measure and travel flows throughout the day gives further guidance on when travel flows align better with location-specific values of time. When available, value of time estimates based on revealed preferences in transportation markets provide a sharper quantification of the relative attractiveness of locations than the use of travel flows alone.

Figure B.6: Relationship between Travel Flows and VOT estimates

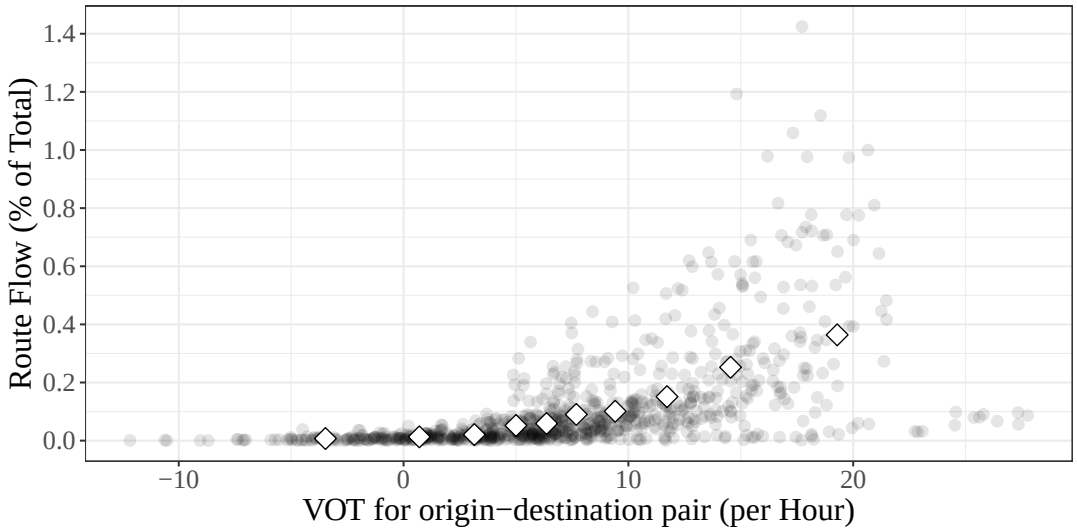

NOTE: Figure B.6 shows the scatter (transparent round dots) and binscatter (white diamonds) relationship between the VOT for an origin-destination pair and the respective traffic flow (as a fraction of the total).

C Driver Supply Side: Omitted Results

C.1 Continuation values: Identification and Estimation

We now discuss further identification results of the supply-side primitives, that is, the time and location-dependent distributions of outside options, $\{\kappa \sim G_t(\cdot|a) : a \in \{1,\dots,A\}, t \in \{1,\dots,T\}\}$. Instead, we observe

(a) the driver request probabilities ρ,

(b) the fee f collected by the platform

(c) the probability of winning the auction with a bid b, denoted by γ,

(d) the conditional distribution of bids by drivers F.

Furthermore, we assume that the discount factor δ is known. We then have the following result:

Proposition 2. *Assume the observables are as listed in items (a)-(d) and the discount factor, δ, is known. Furthermore, assume either of the following conditions hold:*

(i) For each $a \in \{1,\dots,A\}, t \in \{1,\dots,T\}$, there are trips to a with $\tau = 0$.

(ii) For each $a \in \{1,\dots,A\}, t \in \{1,\dots,T\}$, there exists an $\tilde{a} \in \{1,\dots,A\}$ and $\tilde{t} \in \{1,\dots,T\}$, such that there are both trips with $\tau = t - \tilde{t}$ and $\tau = t + 1 - \tilde{t}$ from $\tilde{a}$ to a.

Then, the set of conditional distributions of outside options $\{\kappa \sim G_t(\cdot|a) : a \in \{1,\dots,A\}, t \in \{1,\dots,T\}\}$ *is non-parametrically identified.*

Proof of Proposition 2. Proposition 1 implies that the distribution of $c_{j,t}^{t+\tau}$ is identified, so that

$$c_{j,t}^{t+\tau}(a,\hat{a},\kappa) = \kappa + \delta \cdot \mathbb{E}_{G_{t+1}(\cdot|a)}\left[\mathcal{S}_{j,t+1}(\cdot,a)\right] - \delta^{\tau} \cdot \mathbb{E}_{G_{t+\tau}(\cdot|\hat{a})}\left[\mathcal{S}_{j,t+\tau}(\cdot,\hat{a})\right] \tag{C.1}$$

is known. Under condition (i), for $\tau = 0$, the last two terms drop out and the distribution of outside options κ is therefore directly identified from the cost $c_{j,t}^{t+\tau}(a,\hat{a},\cdot)$.

Dropping the dependence on the driver's index, j, and taking expectations on both sides of Equation C.1 using the distribution of κ conditional on (t,a), $G_t(\cdot|a)$ we obtain:

$$\mathbb{E}_{G_t(\cdot|a_t)}\left[c_t^{t+\tau}(a,\hat{a},\kappa_t)\right] = \mathbb{E}_{G_t(\cdot|a)}\left[\kappa_t\right] + \delta \cdot \mathbb{E}_{G_{t+1}(\cdot|a_t)}\left[\mathcal{S}_{t+1}(\cdot,a)\right] - \delta^{\tau} \cdot \mathbb{E}_{G_{t+\tau}(\cdot|\hat{a})}[\mathcal{S}_{t+\tau}(\cdot,\hat{a})]. \tag{C.2}$$

Under condition (ii), for each $n \geq 0$, a location $\tilde{a}_n$ and a time period t_n exist such that the following hold:

$$\mathbb{E}_{G_{t_n}(\cdot|\tilde{a}_n)}\left[c_{t_n}^{t+n}(\tilde{a}_n,a,\cdot)\right] = \mathbb{E}_{G_{t_n}(\cdot|\tilde{a}_n)}\left[\kappa_{t_n}\right] + \\ \delta \cdot \mathbb{E}_{G_{t_n+1}(\cdot|\tilde{a}_n)}\left[\mathcal{S}_{t_n+1}(\cdot,\tilde{a}_n)\right] - \delta^{t+n-t_n} \cdot \mathbb{E}_{G_{t+n}(\cdot|a)}[\mathcal{S}_{t+n}(\cdot,a)], \tag{C.3}$$

and

$$\mathbb{E}_{G_{t_n}(\cdot|\tilde{a}_n)}\left[c_{t_n}^{t+n+1}(\tilde{a}_n,a,\cdot)\right] = \mathbb{E}_{G_{t_n}(\cdot|\tilde{a}_n)}\left[\kappa_{t_n}\right] + \\ \delta \cdot \mathbb{E}_{G_{t_n+1}(\cdot|\tilde{a}_n)}\left[\mathcal{S}_{t_n+1}(\cdot,\tilde{a}_n)\right] - \delta^{t+n+1-t_n} \cdot \mathbb{E}_{G_{t+n+1}(\cdot|a)}[\mathcal{S}_{t+n+1}(\cdot,a)]. \tag{C.4}$$

Taking the difference between Equation C.3 and Equation C.4, we obtain:

$$\Delta_n \equiv \frac{\mathbb{E}_{G_{t_n}(\cdot|\tilde{a}_n)}\left[c_{t_n}^{t+n}(\tilde{a}_n,a,\cdot)\right] - \mathbb{E}_{G_{t_n}(\cdot|\tilde{a}_n)}\left[c_{t_n}^{t+n+1}(\tilde{a}_n,a,\cdot)\right]}{\delta^{t+n-t_n}} = \\ \delta \cdot \mathbb{E}_{G_{t+n+1}(\cdot|a)}[\mathcal{S}_{t+n+1}(\cdot,a)] - \mathbb{E}_{G_{t+n}(\cdot|a)}[\mathcal{S}_{t+n}(\cdot,a)].$$

Furthermore, note that

$$\Delta_0 + \sum_{n=1}^{T-1} \delta \cdot \Delta_n = \delta \cdot \mathbb{E}_{G_{t+T}(\cdot|a)}[\mathcal{S}_{t+T}(\cdot,a)] - \mathbb{E}_{G_t(\cdot|a)}\left[\mathcal{S}_t(\cdot,a)\right] = (\delta - 1) \cdot \mathbb{E}_{G_t(\cdot|a)}[\mathcal{S}_t(\cdot,a)],$$

where the last equality follows from the stationarity assumption. This identifies $\mathbb{E}_{G_t(\cdot|a)}[\mathcal{S}_t(\cdot,a)]$ and therefore all other unknown expectations for a. We can repeat this procedure for all $a \in \{1,\dots,A\}$. Once the expectations are known, the conditional distributions of κ are directly

identified from the pseudo costs $c_t^{t+\tau}(\cdot)$. □

Estimation: It follows from the proof of Proposition 2 that all driver primitives can be recovered through a simple regression of the pseudo-costs on a set of time- and location-specific dummies. To be precise, given the discount factor and the inferred costs from the GPV inversion at hand, we can run the following regressions in analogy to Equation 15:

$$c_{j,t}^{t+\tau}(a, \hat{a}, \kappa) = \sum_{\tilde{a}\in\{1,\dots,A\}} \sum_{\tilde{t}\in\{1,\dots,T\}} (\mathbb{1}_{\tilde{a}=a,\tilde{t}=t+1} \cdot \delta \cdot \alpha_{\tilde{a},\tilde{t}} - \mathbb{1}_{\tilde{a}=\hat{a},\tilde{t}=\tau+t} \cdot \delta^{\tau} \cdot \alpha_{\tilde{a},\tilde{t}}) + \kappa \tag{C.5}$$

From this we can back out the continuation values as $\mathbb{E}_{G_t(\cdot|a)}[\mathcal{S}_t(\cdot, a)] = \alpha_{a,t}$.

Moreover, the residuals from this regression provide an estimate of the conditional distributions of outside options. So $\hat{\kappa}_{j,t}$ is an estimate of $G_t(\cdot|a)$. With this we can then perform the decomposition of the pseudo costs into a primitive component and a remainder which depends on future cost draws, bids, and locations, $e_{j,t}^{t+\tau}(a, \hat{a}) = c_{j,t}^{t+\tau}(a, \hat{a}) - \kappa_{j,t}$.

C.2 Markups

Figure C.1 shows average markups across hours of the day (Figure C.1a) and location (Figure C.1b):

Figure C.1: Average Markups

(a) By Hour

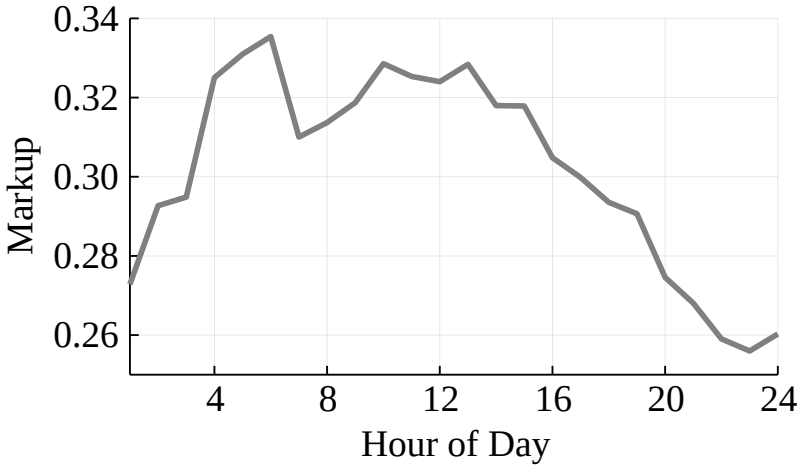

(b) By Location

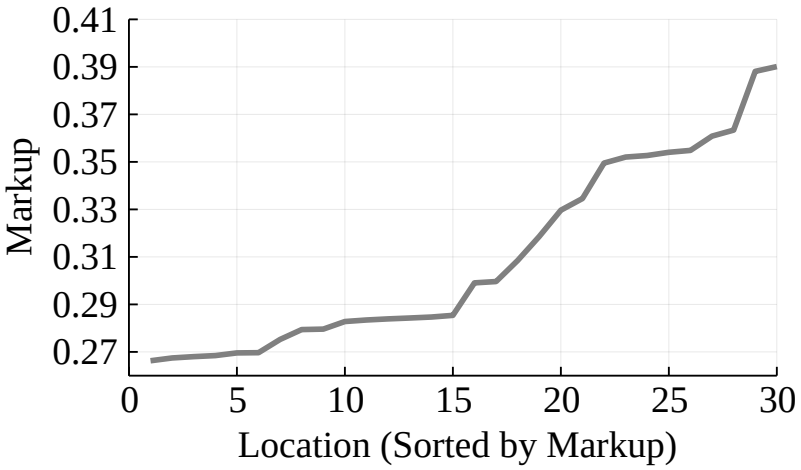

NOTE: Figure C.1 shows average of estimated driver markups by hour (panel C.1a) and location (Figure C.1b). In Figure C.1b, locations are indexed in increasing order of average driver markup.

D Counterfactual Computations

D.1 Platform Policy Function

Here we describe some additional details on the counterfactual implementation:

Selection rule: As described in Section 6, except for menu pricing, the platform's selection rule for depends on the platform's information set. When the platform's information set is $\mathcal{I}$, given a set of drivers J_r, a vector of trip characteristics $\mathbf{z}_r$, and a price vector $\mathbf{p}_r$, the platform would in theory select the driver j that solves $\max_{j \in J_r} \int u_i(p_j, w_{j,t}, \mathbf{x}_{j,t}; \boldsymbol{\beta}) d\Phi(\beta|\mathcal{I})$.

However, for computational reasons, we approximate the platform's selection rule as follows. When the platform's information set is $\mathcal{I}$, let $\overline{\boldsymbol{\beta}}_{\mathcal{I}}$ denote the average consumer parameter under $\Phi(\cdot|\mathcal{I})$. For instance, under uniform pricing, $\overline{\boldsymbol{\beta}}_{\overline{\mathcal{I}}}$ is the *unconditional* expectation of $\boldsymbol{\beta}$, and in third-degree price discrimination by location, $\overline{\boldsymbol{\beta}}_{\mathcal{I}_a}$ is the expectation of $\boldsymbol{\beta}$ *conditional* on the location being a. Given a set of drivers J_r, a vector of trip characteristics $\mathbf{z}_r$, and a price vector $\mathbf{p}_r$, the platform selects the driver j that solves $\max_{j \in J_r} \overline{u}(p_j, w_j, \mathbf{x}_j; \overline{\boldsymbol{\beta}}_{\mathcal{I}})$.

Pricing function: To compute counterfactual equilibria, we need to solve for the platform's pricing function given the platform's selection rule. The pricing function takes the drivers' bids and exogenous trip characteristics and maximizes equation Equation 18. For each counterfactual, we conduct this exercise on a grid of values for the bids and then interpolate linearly between these points to trace out the entire pricing function.

Number of options in counterfactual vs. baseline: The counterfactuals offer the rider fewer alternatives as the platform now preselects the drivers it will offer the consumer according to a selection rule. In comparing consumer surplus, this creates the challenge that consumers earn fewer T1EV draws counterfactually, leading to a mechanical decline in consumer surplus. To eliminate this effect, we keep the number of offers the same as in the baseline scenario. For instance, a consumer who in the baseline mechanism receives n_r offers is presented with n_r identical options in the uniform pricing counterfactual to keep consumer surplus from the unobservable iid utility shifters ϵ constant.

D.2 Equilibrium Computation

This section describes how we compute the counterfactual bid distribution of drivers. Note that the key equilibrium object is $\gamma(\cdot|a_t, \mathbf{z}_j)$, where $\mathbf{z}_j$ includes persistent driver-specific attributes, such as rating and car type. As we explain in the main text, these objects at baseline depend on

the consumer preferences. It also includes the wait time, which we hold fixed since we are not changing the matching process. These attributes make this an asymmetric auction.

In the counterfactual, the platform uses a selection rule S to pick the driver that ultimately serves the ride, so that the winning probability depends on S, $\gamma(\cdot|a_t, \mathbf{z}_j; S)$. To make the counterfactual computation tractable, instead of solving a complicated set of differential equations, we let drivers re-optimize their bids on a very fine grid. With a new set of bids for every driver we can then update to a new version of $\gamma^k(\cdot|a_t, \mathbf{z}_j; S)$, which is again simulated as we describe in the main text. For the simulation of $\gamma^k(\cdot|a_t, \mathbf{z}_j)$ we condition on a_t and then take seventy draws of each of the bids in our grid $\mathcal{B}_g$. We then update bids according to a weighted average of the old and the new bid with $\phi = 0.75$ placed on the new bid and $1 - \phi = 0.25$ on the old bid. This smooths out the updating and leads to better convergence. In Table D.1 we describe the algorithm in detail.

Table D.1: Algorithm for Counterfactual Bid Distribution of Drivers

Algorithm 1: Computing Counterfactual Bid Distribution

Result: Computation of $\mathbf{b}$

while $\|\mathbf{b}^k - \mathbf{b}^{k+1}\| >$ `outer_tolerance` **do**

  for $r = 1$ *to* N_r, $j \in \mathcal{J}_r$ **do**

    Initialize: $b_{\max} = -\infty$

    for $b \in \mathcal{B}_g$ **do**

      $\gamma^{k-1}(b|a_t, \mathbf{z}_j) = 0$

      for $s = 1$ *to* N_s **do**

        $\gamma^{k-1}(b|a_t, \mathbf{z}_j) =$
        $\gamma^{k-1}(b|a_t, \mathbf{z}_j) + \frac{1}{N_s} \cdot \mathbf{1}\cdot\{\text{Bid is offered to consumer under } S \text{ and accepted at } p_j(b)\}$

      end

    end

    $b_{\max} = \arg\max_{x \in \{b, b_{\max}\}} \gamma^{k-1}(x|a_t, \mathbf{z}_j) \cdot \left(x - c_j\right)$;

  end

  $b^k_{rj} = b_{\max} \cdot \phi \cdot b^{k-1}_{rj} \cdot (1 - \phi)$;

end

D.3 Price Heterogeneity under Third Degree Price Discrimination

We provide more detail on the hourly and location-wise variation of the platform prices under time-of-day and location-based third degree price discrimination.

Figure D.1a shows the results for third degree price discrimination by time of day. The black line shows prices by hour when the platform conditions pricing on the hour of day. We can see that hour by hour price variation is relatively minor with prices ranging between slightly less than twelve and slightly more than thirteen dollars. Similarly, the dotted black line also shows prices under the hypothetical scenario where the input price (from the driver that maximizes average consumer preferences) is held constant at the average daily input price. Under constant input prices, there is even less heterogeneity. Indeed, the solid black line very closely tracks the average input price, which suggests that the platform passes through the inter-temporal cost variation from drivers but otherwise does not adjust prices much throughout the day for demand side reasons.

Figure D.1b shows a similar pattern exists for third degree price discrimination by location. There are differences in prices by location but these closely track changes in driver cost. Hypothetical prices under constant input prices across space vary very little.

Figure D.1: Average Prices in Third-Degree Price Discrimination

(a) By Time of Day

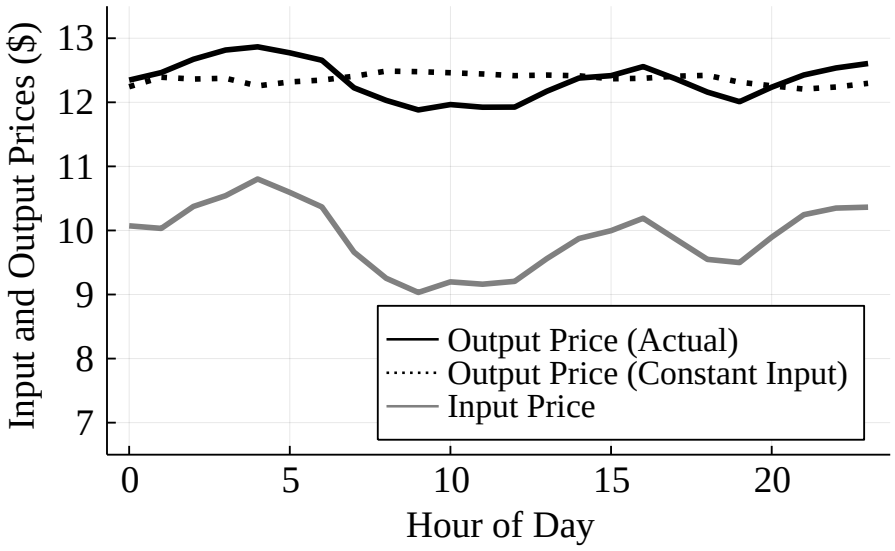

(b) By Location

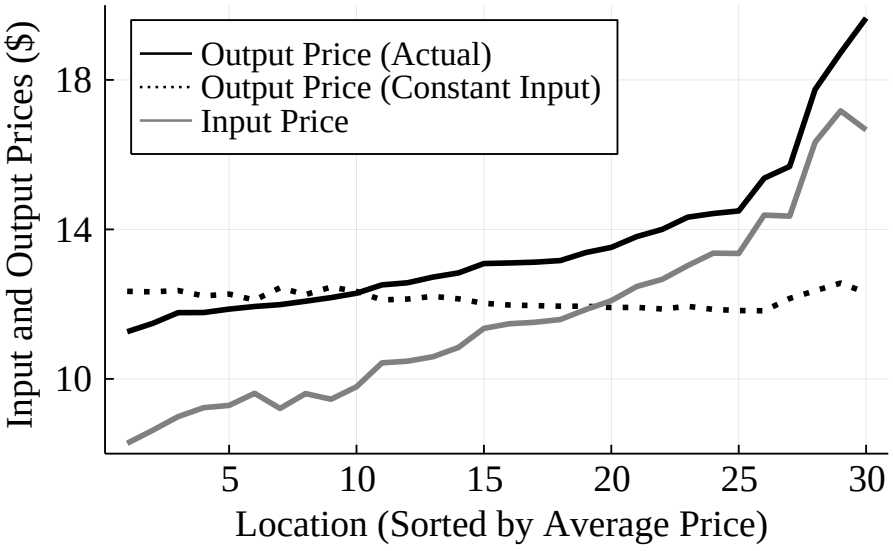

NOTE: In Figure D.1a, the solid black line shows average prices by hour under third degree price discrimination by time-of-day. The gray line shows average input prices and the dotted black line average prices by hour when the input price is held constant throughout the day at the daily average input price. Similarly, Figure D.1b shows average prices by location under third degree price discrimination by location. The gray line shows average input prices across location and the dotted black line average prices by location when the input price is held constant across locations at average input price.

D.4 Counterfactual Bounding Exercise to Driver Cost Changes

We describe in this section how we probe the robustness of our counterfactual results in Section 6 to changes in the drivers' continuation values. To do so, we leverage Proposition 2, which requires that we assume a discount factor. We choose $\delta = 1 - 0.0625$. Interpreting δ as the probability that the shift randomly terminates, $\delta = 1 - 0.0625$ corresponds to an average remaining shift length of four hours, which is about half of a taxi driver's typical workday. With the discount factor and the inferred costs from the GPV inversion at hand, we run the regression described in Equation C.5, to back out continuation values and outside options.

In principle, the results in Proposition 2 allow us to recompute $e_{j,t}$ for each candidate equilibrium of drivers bids conditional on the platforms pricing policy. However, even without re-computing $e_{j,t}$ it takes several days to compute equilibria. Thus, the analysis of a full dynamic adjustment of drivers' bids and value functions is outside of the scope of the current paper.

Instead, we probe the robustness of our counterfactual results to a change in the endogenous portion of the cost by the following exercise. Because drivers are losing revenue under all alternative pricing equilibria, we let $c_{j,t} = \kappa_{j,t} + 1.1 \cdot e_{j,t}$. That is, we recompute equilibria under a ten percent increase of the endogenous cost. This is a relatively large change and we expect the actual counterfactual change in e to be smaller as it includes both endogenous future bids and allocations but also exogenous future outside option draws κ. Hence, we interpret the results from this exercise as an upper bound on the counterfactual changes from the adjustments in continuation values.

Table D.2 shows the results from this exercise. The results show that the increase in driver costs is passed on to consumers, which leads to slightly higher prices in all counterfactuals. This means that driver surplus, consumer surplus, and platform profits are slightly lower. However, despite these changes, whose direction we would have anticipated, the qualitative predictions from the previous counterfactuals hold. The platform does not benefit from pricing by location or time relative to uniform pricing. Personalized pricing is still by far the most profitable pricing strategy for the platform and like before, the proportion of trips served by the platform vary very little across these counterfactuals.

Table D.2: Price Discrimination Counterfactual Results: Bounding Exercise

Pricing Type	Avg. Platform Price	Surcharge	Driver Bid	Inside Option	Platform Profits per Order	Driver Profits per Order	Consumer Surplus	Average VOT Accepted Ride
Baseline (10% flat fee)	$9.83	-	$8.84	0.655	$0.55	$1.67	$1.29	$14.27
Uniform Pricing								
No Driver Adjustment	$11.13	-	$8.84	0.38	$1.12	$0.7	$0.79	$15.17
Driver Adjustment	$11.71	-	$10.42	0.31	$0.9	$0.8	$0.62	$15.41
Third-degree by Location								
No Driver Adjustment	$11.17	-	$8.84	0.382	$1.11	$0.728	$0.78	$15.14
Driver Adjustment	$11.89	-	$10.34	0.31	$0.89	$0.8	$0.62	$15.38
Third-degree by Hour								
No Driver Adjustment	$11.14	-	$8.84	0.383	$1.11	$0.702	$0.78	$15.15
Driver Adjustment	$11.75	-	$10.42	0.31	$0.84	$0.8	$0.61	$15.38
Menu Pricing								
No Driver Adjustment	$10.36	$0.84	$8.84	0.358	$1.0	$1.12	$0.71	$15.21
Driver Adjustment	$11.58	$1.25	$10.68	0.31	$0.87	$1.19	$0.61	$15.24
Personalized Pricing								
No Driver Adjustment	$11.18	-	$8.84	0.435	$2.31	$0.717	$0.82	$14.58
Driver Adjustment	$12.98	-	$10.51	0.31	$1.66	$0.83	$0.56	$14.93

Note: Table D.2 summarizes the results of the pricing counterfactuals in the bounding exercise outlined in Appendix D.4.